# CALCULATION SUMMARY SHEET



PROJECT NUMBER: 143418

PROJECT NAME: USEN – Trench 13 Design

DATE: March 25th, 2015

CALCULATION NUMBER: C.10 Revision: 1 (March 11, 2016)

**CALCULATION TITLE: Anchor Trench Dimensions**

**DESCRIPTION OF CALCULATION:**

Calculation to determine required anchor trench dimensions for Trench 13

**REFERENCES USED:** Number of Reference Pages Attached:

1-5 Technical Journals for Interpretation of Friction Angles of Geosynthetics

6. Koerner, Robert M. *Designing with Geosynthetics ( 3rd Edition 1994) Anchor Trench Design*

7. Product Specifications for Geosynthetic Clay Liners

**REVIEW COMMENTS:**

.

| | | | |
|---|---|---|---|
| CALCULATION MADE BY: | CWK | DATE: | 3/25/15 |
| CALCULATION CHECKED BY: | PAZ | DATE: | 04/27/15 |
| CALCULATION REVISED BY: | CWK | DATE: | 04/28/15 |
| CALCULATION REVIEWED BY: | CAB | DATE: | 4/28/15 |

## PURPOSE OF CALCULATION

To evaluated the tensile strength capacity of the anchor trench for Trench 13 liner system, and provided basis for the specified dimensions of the anchor trench.

## METHOD

The tensile strength capacity of the anchor trench is evaluated using the methodology presents in Koerner (1994) *Designing with Geosynthetics*. The methodology is based on a static equilibrium analysis of the frictional forces acting on the liner system.

## APPROACH

- Assume tension in liner system is taken by the sum of the frictions resistance in the anchor trench.
- Illustrated in the diagram below, assume frictionless pulleys at angle points in order to simplify analysis.

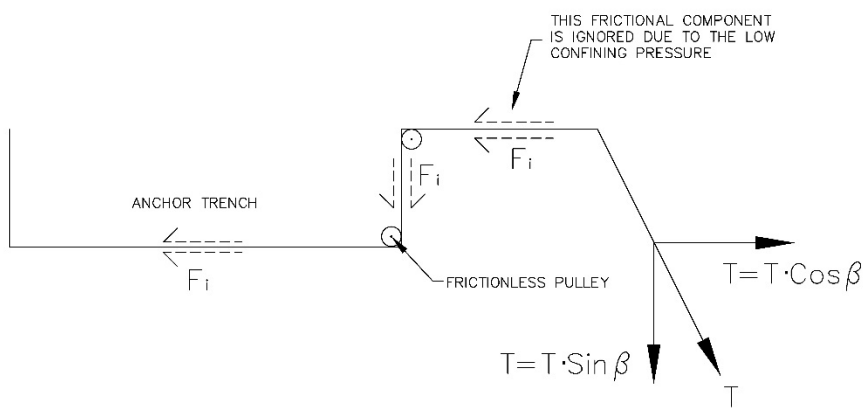


- $F_i$ = Resistance along soil/liner system interface
- Maximum tension from the liner system due to gravity, wind uplift, seismic deformation, and waste settlement were determined in the *Liner Stability on Trench 13 Side Slopes Calculation* (**Calculation C.09***).*
- Friction angles between interfaces of liner components and compacted backfill are determined from technical journals provided in the reference section of this calculation.
- Frictional components will be split into three zones, in order of depth within the anchor trench. Figure 1 illustrates the separation of liner components and orientation of those components in the anchor trench. Figure 2 is a free body diagram of the frictional forces due to weight of compacted backfill and tensile force acting on liner system. The entire system is assumed to be in static equilibrium.

- The analysis is to demonstrate that the anchor trench is adequate to hold the liner material against pullout. While literature commonly reports a preference for pullout before liner failure, these are for shallow angle slopes, where the liner edge could be recovered and reburied if necessary. For the US Ecology site, a trench pullout could be challenging to recover because of the steepness of the slope. The preferred option is for spot repair of liner failure, if necessary.

- Wind loading is not considered in this analysis because of the complexity of the forces involved. The construction specification will require adequate anchoring of the liner components to prevent uplift.

**Initial Assumptions for Geometry of Anchor Trench: L1 = 10 ft; L2 = 5 ft; H1 = 2 ft; H2 = 1 ft; and H3 = 1 ft**

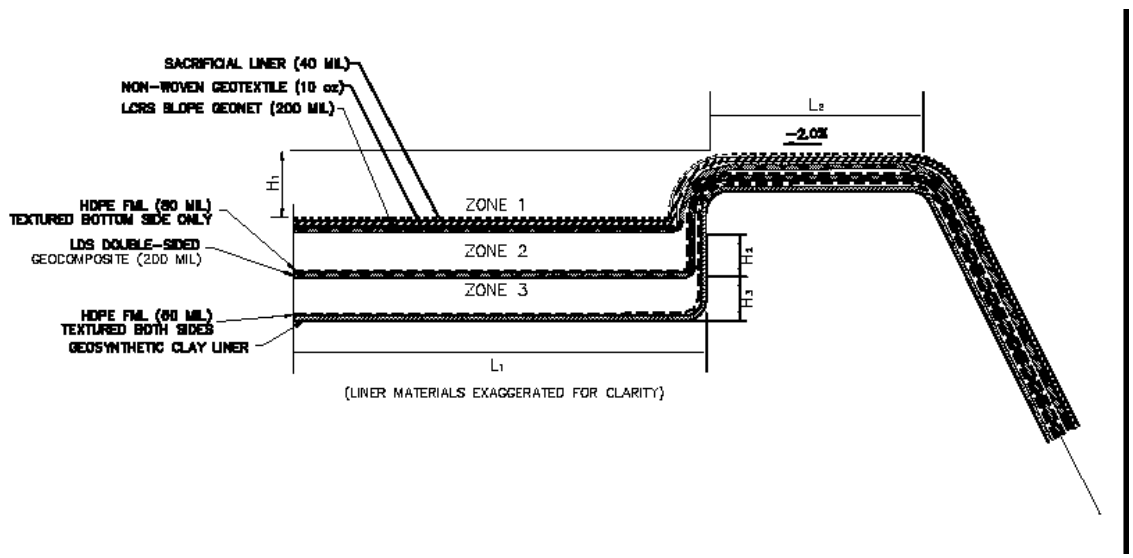


**Various Forces Acting on the Liner System**

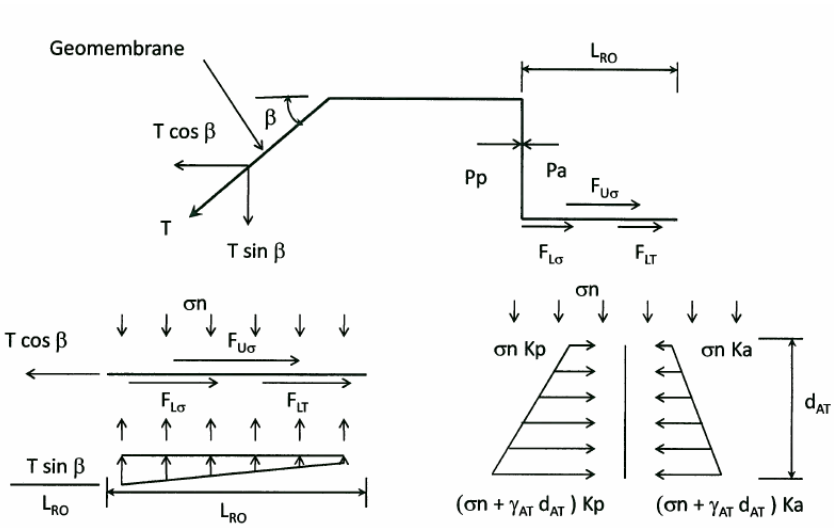

Equations taken from *Koerner – Designing with Geosynthetics* – Included as **Reference 6**.

$$\sum F_X = 0$$

$$\mathbf{T_{allowable} * \cos\beta = F_{U\sigma} + F_{L\sigma} + F_{LT} - P_a + P_p}$$

Where:

$T_{allowable}$ = allowable tensile force on liner system
$\beta$ = tension force angle
$F_{U\sigma}$ = shear force above liner system due to compacted backfill
$F_{L\sigma}$ = shear force below liner system due to compacted backfill
$F_{LT}$ = shear force below liner system due to vertical component of $T_{allowable}$
$P_a$ = active earth pressure against the side of the anchor trench
$P_p$ = passive earth pressure against the in-situ side of the anchor trench
$L_{ro}$ = horizontal length of anchor trench

The shear force below the liner system due to the vertical component of $T_{allowable}$ is defined as:

$$F_{LT} = T_{allowable} \sin\beta \, tan\delta$$

## Zone 1

Material Properties:

Values for total tensile load were calculated in Table 3 of the Liner *Stability on Trench 13 Side Slopes* (**Calculation C.09**) calculation.

**Yield Strength of Liner Members in Zone 1**

| Material | Yield Strength | Strain (elongation) at Yield |
|---|---|---|
| | *(lb/in)* | *%* |
| Sacrificial 40 Mil HDPE Liner | 84 | 12 |
| 10oz Non-woven Geotextile | 150 | 50 |
| Geonet – LCRS Side Slope – 220 Mil | 45 | 23 |

Note: Reference is **Calculation C.09**.

The maximum yield strength for the combined liner members located in Zone 1 is the sum of the tensile strengths at the failure of the weakest member. Stress-strain graphs were not available for each liner component, so the maximum tensile strength for the liner components was selected for the strongest component, or 150 lbs/in or 1800 lbs/ft for the geotextile. This value is used to determine if the dimensions of the anchor trench meet the required capacity to prevent pull-out.

Friction angles for the interface between liner materials and the soil backfill / other liner members were referenced from multiple technical journals located in the references of this calculation. In the case of Zone 1, the upper shear force will have an interface between the compacted backfill and the sacrificial liner, the lower shear force will have

an interface between the geonet and compacted backfill, and the weakest interface angle between the liner materials in Zone 1 is between the sacrificial liner and the geonet.

| **Material** | **Friction Angle ($\delta$)** | **Reference** |
|---|---|---|
| | *deg* | # |
| Sacrificial Liner 40 Mil Smooth HDPE Liner and Sand | 23.6 | 3 |
| Sacrificial Liner 40 Mil Smooth HDPE and 10oz Non-woven Geotextile | 15.1 | 3 |
| 10oz Non-woven Geotextile and Geonet – LCRS Side Slope – 200 Mil | 24.5 | 2 |
| Geonet – LCRS Side Slope – 200 Mil and Sand | 21 | 4 |

Soil Properties:

The entire anchor trench will be composed compacted backfill which will have the following properties:

$\boldsymbol{\gamma}$ = density = 120 $\frac{lb}{ft^3}$

$\boldsymbol{\delta}$ = internal angle of friction = 35° (Reference from **Calculation C.09**)

$\boldsymbol{\sigma_n}$ = normal force = $\gamma * depth\ of\ Zone\ 1\ (H1) = 120 * 2 = 240 \frac{lb}{ft^2}$

The backfill in the anchor trench (L1 on Figure 1) will be the only soil holding the liner in-place and the only normal force considered in this calculation. The liner at L2 and side slopes in Figure 1 will remain exposed until final cover placement. Therefore, there is no additional normal loading included in the calculation.

Force Analysis

Upper shear force between the soil and sacrificial liner:

$$F_{U\sigma} = \sigma_n * tan\delta * L$$

The weakest interface friction angle in Zone 1 will be controlling which occurs between the sacrificial liner and the geotextile, that angle is 15.1 degrees.

$$F_{U\sigma} = 240 \frac{lb}{ft^2} * tan(15.1) * 10ft = 647.6 = 650 \frac{lb}{ft}$$

Lower shear force between the geonet and compacted backfill:

$$F_{L\sigma} = \sigma_n * \tan\delta * L$$

However, the weakest interface friction angle in Zone 1 will be controlling, which occurs between the sacrificial liner and the geotextile, (15.1 degrees). Therefore, the lower friction stress contribution $F_{L\sigma}$ is computed using that angle, rather than the friction angle between the lowest member (geonet) and the trench backfill material. Therefore, $F_{L\sigma} = F_{U\sigma}$ =650 lb/ft.

Active earth pressure (see Figure 2 for illustration and **Reference 6**):

The internal frictional angle of the compacted backfill is 35 degrees.

$$K_a = [\tan\left(45 - \frac{\varphi}{2}\right)]^2 = (\tan 27.5)^2 = 0.27$$

$$P_a = \frac{1}{2} * \gamma * {H_1}^2 * K_a = \frac{1}{2} * 120 \frac{\text{lb}}{\text{ft}^3} * (2\text{ ft})^2 * 0.27 = 64.8 = 65\ \frac{\text{lb}}{\text{ft}}$$

Passive earth pressure (see Figure 2 for illustration and **Reference 6**):

The internal frictional angle of the compacted backfill is 35 degrees.

$$K_p = [\tan\left(45 + \frac{\varphi}{2}\right)]^2 = (\tan 62.5)^2 = 3.69$$

$$P_p = \frac{1}{2} * \gamma * {H_1}^2 * K_p = \frac{1}{2} * 120 \frac{\text{lb}}{\text{ft}^3} * (2\text{ ft})^2 * 3.69 = 885.6 = 890\ \frac{\text{lb}}{\text{ft}}$$

Allowable tensile force in Zone 1:

$$T_{\text{allowable}} \cos\beta = F_{U\sigma} + F_{L\sigma} + F_{LT} - P_a + P_p$$

$$F_{LT} = T_{\text{allowable}} \sin\beta\, tan\delta$$

Rewrite the equation to have T allowable on the left hand side:

$$T_{\text{allowable}} = \frac{F_{U\sigma} + F_{L\sigma} - P_a + P_p}{\cos\beta - \sin\beta * \tan\delta}$$

The angle of resultant tension in the liner components for Zone 1 is beta, 63.4 degrees. The weakest interface angle in Zone 1 is delta, 15.1 degrees.

$$T_{\text{allowable}} = \frac{650 + 650 - 65 + 890}{\cos 63.4 - \sin 63.4 * \tan 15.1}$$

$$T_{\text{allowable}} = \frac{2125}{.21} = 10{,}119 = 10{,}000\ \frac{lb}{ft} = 10.0 \frac{kips}{ft}$$

The maximum tensile load for all liner components in Zone 1 is 1800 lb/ft which is less than the allowable tension of 10,000 lb/ft, providing a factor of safety of 5.6.

## Zone 2

Material Properties:

### Yield Strength of Liner Members in Zone 2

| Material | Yield Strength | Strain (elongation) at Yield |
|---|---|---|
| | *(lb/in)* | *%* |
| 80 Mil HDPE Single Sided Texture | 176 | 13 |
| LDS Side Slope Geocomposite 6 oz double-sided 200 mil | 50 | 50 |

Note: Reference is Calculation C.09.

The maximum yield strength for a liner members located in Zone 2 of the anchor trench is 176 lbs/in or 2,112 lbs/ft and this value is used to determine if the dimensions of the anchor trench meet the required capacity to prevent pull-out.

Friction angles for the interface between liner materials and the soil backfill / other liner members are referenced from journals and technical reports and are attached as references to this calculation. In the case of Zone 2, the upper shear force will have an interface between the compacted backfill and the 80 mil smooth HDPE Geomembrane, the lower shear force will have and interface between the LDS 200 mil Geocomposite and compacted backfill.

| Material | Friction Angle ($\delta$) | Reference |
|---|---|---|
| | *deg* | # |
| 80 Mil HDPE Single Sided Smooth Upper Surface and Sand | 23.3 | 3 |
| 80 Mil HDPE Single Sided Texture Lower Surface and LDS Side Slope Geocomposite 6 oz double-sided 200 mil | 32.1 | 5 |
| LDS Side Slope Geocomposite 6 oz double-sided 200 mil and Sand | 21 | 4 |

Soil Properties:

The entire anchor trench will be composed of re-compacted soil which will have the following properties:

$\boldsymbol{\gamma}$ = density = 120 $\frac{lb}{ft^3}$

$\boldsymbol{\delta}$ = internal angle of friction = 35°

$\boldsymbol{\sigma_n}$ = normal force = $\gamma * (H1 + H2) = 120 * (2 + 1) = 360 \frac{lb}{ft^2}$

Force Analysis

Upper shear force between the soil and smooth HDPE:

$$F_{U\sigma} = \sigma_n * tan\delta * L$$

The weakest interface friction angle in Zone 2 will be controlling, which occurs between the geocomposite and compacted backfill, at 21 degrees.

$$F_{U\sigma} = 360\frac{\text{lb}}{\text{ft}^2} * tan(21) * 10ft = 1381.9 = 1400\frac{\text{lb}}{\text{ft}}$$

Lower shear force between the 200 mil LDS Geocomposite and soil:

$$F_{L\sigma} = \sigma_n * tan\delta * L$$

And is the same as $F_{U\sigma}$ or 1400 lb/ft.

Active earth pressure:

The internal frictional angle of the compacted backfill is 35 degrees.

$$K_a = [\tan\left(45 - \frac{\varphi}{2}\right)]^2 = (\tan 27.5)^2 = 0.27$$

$$P_a = \left(\frac{1}{2} * \gamma * (H_2)^2 * K_a\right) + (\gamma * (H_1 + H_2)^2 * K_a) = \left(\frac{1}{2} * 120\frac{\text{lb}}{\text{ft}^3} * (1\text{ft})^2 * 0.27\right) + \left(120\frac{\text{lb}}{\text{ft}^3} * (3\text{ft})^2 * 0.27\right)$$
$$= 307.8\frac{\text{lb}}{\text{ft}} = 310\frac{\text{lb}}{\text{ft}}$$

Passive earth pressure:

The internal frictional angle of the compacted backfill is 35 degrees.

$$K_p = [\tan\left(45 + \frac{\varphi}{2}\right)]^2 = (\tan 62.5)^2 = 3.69$$

$$P_p = \left(\frac{1}{2} * \gamma * {H_2}^2 * K_p\right) + \left(\gamma * (H_1 + H_2)^2 * K_p\right) = \left(\frac{1}{2} * 120\frac{\text{lb}}{\text{ft}^3} * (1\text{ ft})^2 * 3.69\right) + \left(120\frac{\text{lb}}{\text{ft}^3} * (3\text{ ft})^2 * 3.69\right) =$$
$$4{,}206.6\ \frac{\text{lb}}{\text{ft}}\ \text{or}\ 4200\frac{lb}{ft}$$

Allowable tensile force in Zone 2 (as previously defined):

$$T_{\text{allowable}} = \frac{F_{U\sigma} + F_{L\sigma} - P_a + P_p}{\cos\beta - \sin\beta * tan\delta}$$

The angle of resultant tension in the liner components for Zone 2 is beta, 63.4 degrees (see Figure 3). The weakest interface angle in Zone 2 is delta, 21 degrees.

$$T_{\text{allowable}} = \frac{1400 + 1400 - 310 + 4200}{\cos 63.4 - \sin 63.4 * \tan 21}$$

$$T_{allowable} = \frac{6690}{0.10} = 66{,}900\frac{lb}{ft} = 67\ \frac{kips}{ft}$$

The maximum tensile load for all liner components in Zone 2 is 2,112 lb/ft which is less than the allowable tension of 67, 000 lb/ft, providing a factor of safety of 32.

**Zone 3**

Material Properties:

**Yield Strength of Liner Members in Zone 3**

| Material | Yield Strength | Strain (elongation) at Yield |
|---|---|---|
| | *(lb/in)* | *%* |
| 60 Mil HDPE Double Sided Texture | 132 | 13 |
| Geosynthetic Clay Liner | 50 | 15 |

Note: Reference is **Calculation C.09**.

The maximum yield strength for liner members located in Zone 3 of the anchor trench is 132 lbs/in or 1,584 lbs/ft and is used to determine if the dimensions of the anchor trench meet the required capacity to prevent pull-out.

Friction angles for the interface between liner materials and the soil backfill / other liner members are attached as references to this calculation. In the case of Zone 3, the upper shear force will have an interface between the backfill soil and the 60 mil textured HDPE Geomembrane, the lower shear force will have and interface between the Geosynthetic Clay Liner and backfill soil, and the weakest interface angle is between the two liner materials in Zone 3.

| Material | Friction Angle ($\delta$) | Reference |
|---|---|---|
| | *deg°* | # |
| 60 Mil HDPE Double Sided Texture and Sand | 36.6 | 3 |
| 60 Mil HDPE Double Sided Texture and Geosynthetic Clay Liner | 24 | 7 |
| Geosynthetic Clay Liner and Sand | 35.6 | 1 |

Soil Properties:

The entire anchor trench will be composed of re-compacted soil which will have the following properties:

$\gamma$ = density = 120 $\frac{lb}{ft^3}$

$\delta$ = internal angle of friction = 35°

$\boldsymbol{\sigma_n}$ = normal force = $\gamma * (H1 + H2 + H3) = 120 * (2 + 1 + 1) = 480\frac{lb}{ft^2}$

Force Analysis

Upper shear force between the soil and 60 Mil textured HDPE:

$$F_{U\sigma} = \sigma_n * tan\delta * L$$

The weakest interface friction angle in Zone 3 will be controlling, which occurs between the textured HDPE and GCL, that angle is 23.4 degrees.

$$F_{U\sigma} = 480\,\frac{lb}{ft^2} * tan(24) * 10ft = 2137.1 = 2100\,\frac{lb}{ft}$$

Lower shear force between the Geosynthetic Clay Liner and soil:

$$F_{L\sigma} = \sigma_n * tan\delta * L$$

The weakest interface friction angle in Zone 3 will be controlling, which occurs between the textured HDPE and GCL, that angle is 23.4 degrees. Therefore $F_{L\sigma} = F_{U\sigma} = 2100$ lb/ft.

Active earth pressure:

The internal frictional angle of the compacted backfill is 35 degrees.

$$\mathrm{K_a} = [\tan\left(45 - \frac{\varphi}{2}\right)]^2 = (\tan 27.5)^2 = 0.27$$

$$\mathrm{P_a} = \left(\frac{1}{2} * \gamma * {H_3}^2 * \mathrm{K_a}\right) + (\gamma * (H_1 + H_2 + H_3)^2 * \mathrm{K_a})$$

$$= \left(\frac{1}{2} * 120\,\frac{\mathrm{lb}}{\mathrm{ft}^3} * (1\mathrm{ft})^2 * 0.27\right) + \left(120\,\frac{\mathrm{lb}}{\mathrm{ft}^3} * (4\mathrm{ft})^2 * 0.27\right) = 534.6 = 530\,\frac{\mathrm{lb}}{\mathrm{ft}}$$

Passive earth pressure:

The internal frictional angle of the compacted backfill is 35 degrees.

$$\mathrm{K_p} = [\tan\left(45 + \frac{\varphi}{2}\right)]^2 = (\tan 62.5)^2 = 3.69$$

$$\mathrm{P_p} = \left(\frac{1}{2} * \gamma * {H_3}^2 * \mathrm{K_p}\right) + \left(\gamma * (H_1 + H_2 + \mathrm{H_3})^2 * \mathrm{K_p}\right)$$

$$= \left(\frac{1}{2} * 120\,\frac{\mathrm{lb}}{\mathrm{ft}^3} * (1\ \mathrm{ft})^2 * 3.69\right) + \left(120\,\frac{\mathrm{lb}}{\mathrm{ft}^3} * (4\ \mathrm{ft})^2 * 3.69\right) = 7306.2 = 7300\,\frac{\mathrm{lb}}{\mathrm{ft}}$$

Allowable tensile force in Zone 3 (as previously defined):

$$\mathrm{T_{allowable}} = \frac{F_{U\sigma} + F_{L\sigma} - P_a + P_p}{\cos\beta - \sin\beta * tan\delta}$$

The angle of resultant tension in the liner components for Zone 3 is beta, 63.4 degrees. The weakest interface angle in Zone 2 is delta, 24 degrees.

$$T_{allowable} = \frac{2100 + 2100 - 530 + 7300}{\cos 63.4 - \sin 63.4 * \tan 24}$$

$$T_{allowable} = \frac{10{,}970}{.05} = 219{,}400 \frac{lb}{ft} = 220 \frac{kips}{ft}$$

The maximum tensile load for all liner components in Zone 3 is 1,584 lb/ft which is less than the allowable tension of 220,000 lb/ft, providing a factor of safety of 139.

## SUMMARY

According to these analyses the anchor trench will provide sufficient resistance to the forces developed in the liner system. The anchor trench is designed for the liner members to fail in extreme tension rather than pull out of the anchor trench. The table below summarizes the results from the analysis above.

| **Zone** | **Liner Members** | **Maximum Yield Strength** | **Allowable Tensile Load** | **Factor of Safety Against Pull-out** |
|---|---|---|---|---|
| # | | *lb/ft* | *lb/ft* | |
| 1 | Sacrificial Liner -30 Mil Smooth HDPE<br>Non-Woven Geotextile – 10 oz<br>LCRS Side-Slope Geonet 200 Mil | 1,800 | 10,000 | 5.6 |
| 2 | 80 Mil HDPE Geomembrane (textured bottom side)<br>LDS Side-Slope Geocomposite 200 Mil | 2,112 | 67,000 | 32 |
| 3 | 60 Mil HDPE Geomembrane (textured both sides)<br>Geosynthetic Clay Liner | 1,584 | 220,000 | 139 |

REFERENCE 1

Scientia Iranica A (2012) 19 (4), 1044–1051

Sharif University of Technology

**Scientia Iranica**

*Transactions A: Civil Engineering*

www.sciencedirect.com

Research note

# Mechanical behaviour of sand-geotextile interface

**S.C. Tuna** *, **S. Altun**

*Department of Civil Engineering, Ege University, 35100, Bornova - Izmir, Turkey*

Received 2 January 2012; revised 16 February 2012; accepted 28 April 2012

**KEYWORDS**

Geotextiles;
Interface behaviour;
Direct shear test;
Sand.

**Abstract** In this study, interface direct shear tests were undertaken to investigate improvement in the mechanical behaviour of granular soils when reinforced with geotextile inclusions. Unlike past studies, various different parameters were investigated in the same study to uncover more assuring results. As expected, the interface friction angle of the reinforced sand was found to be lower than that of the unreinforced sand. No remarkable difference was seen in the shear strength of reinforced and unreinforced sands, but in reinforced sand, there was no post-peak loss of strength, as seen in unreinforced sand. Unexpectedly, geotextile inclusions did not restrict the soil from dilating. If the geotextile content was increased in the test specimen, only then did the dilation of the sand decrease. At the end of the results, it was concluded that the interface behaviour depends on the combined effects of the surface properties and deformability of the geotextiles, and also on the index properties of the soil.

© 2012 Sharif University of Technology. Production and hosting by Elsevier B.V.
Open access under CC BY-NC-ND license.

## 1. Introduction

Composite materials combine the strength of two or more different materials in a supplementary way and are extensively used in different fields of engineering. From the same point of view, reinforcements in soil have been extensively used from Bablyonian times. Reinforcements enhance the tensile force capacity of the composite system, thus reducing the probability of potential failure and increasing overall capacity. Nowadays, geosynthetic reinforcements are used as an alternative design material, especially considering their environmental and economical superiority in nearly all civil engineering fields.

The interaction between soils and geosynthetics plays an important role in general stability concerns. Thus, interface behavior is one of the important factors in the design of structures in order to check the internal stability of geosynthetic-reinforced soils. There are two most important failure criteria to be analysed in geosynthetic-reinforced soils [1]: (1) Pull-out mode of failure; (2) sliding mode of failure. In the direct shear mode of failure, there is a plane of weakness around the geosynthetics inclusion because of the shear strength loss of the soil in the interface region. These two modes are interrelated; in the pull-out mode, there is a direct application of tensile force to the specimen (the design philosophy used in geosynthetic retaining walls and slopes), and on the other hand in the direct shear mode, the weakness of the interface region plays an important part. From the related literature survey, one can state that the soil–geosynthetic interaction parameters are influenced by:

(a) The interaction mechanism between geomaterials and geosynthetics.
(b) Physical and mechanical properties of geomaterials (density, grain shape and size, grain size distribution, etc.).
(c) Mechanical properties (tensile peak strength), geometry and surface properties of geosynthetics.

In the past, pull-out [2], triaxial compression [3], direct shear [4,5], ring shear [6] and some other modified tests [7–9] have been performed, to analyse the mechanical behaviour of reinforced soils. Takasumi et al. [10] suggest that the direct shear test is appropriate for evaluating the strength characteristics of the soil–geosynthetic interface, if the extensibility of the geosynthetic does not affect its field performance.

Soil–geosynthetics interface behaviour generally depends on particle size and/or particle-surface mechanical interaction behaviour. With this in mind, there are two types of interface

* Corresponding author. Tel.: +90 232 3886026.
*E-mail addresses:* tunasahincaglar@hotmail.com (S.C. Tuna), selim.altun@ege.edu.tr (S. Altun).

Peer review under responsibility of Sharif University of Technology.

Production and hosting by Elsevier

1026-3098 © 2012 Sharif University of Technology. Production and hosting by Elsevier B.V. Open access under CC BY-NC-ND license.
doi:10.1016/j.scient.2012.06.009

behaviour stated [11] in the literature; one is a dilative system, and the other is a non-dilative system. On the other hand, in reality, systems are generally inbetween these two separate types. Frost et al. [12] extensively researched the governing mechanisms that effect interface shear behaviour and strength. They demonstrated the coupled effect of surface hardness and roughness, together with normal stress, by performing laboratory tests of sand-continuum material interfaces (soil-concrete, soil-geomembrane, soil-steel etc.) and through the discrete element modelling of these interfaces.

Therefore, the purpose of this study should include the following:

(a) Reinforced soil interface behaviour has been widely analysed in the past, and different results have shown the interface behaviour of geosynthetics-reinforced soils. In all studies, only the effect of one or two parameters are investigated, thus, behaviors are not precisely specified. In this study, various parameters are investigated to have a clear idea about the topic.
(b) To use different types of geomaterial and geosynthetics to investigate the effects of important parameters on the behaviour of the interface system [13].

## 2. Experimental program

An experimental program involving over 95 direct shear tests was performed to characterize the friction properties existing at the sand-geotextile interface.

The testing apparatus consisted of a 60 mm ∗ 60 mm and a 100 mm ∗ 100 mm square shear box with a displacement-controlled system operating at 100–250 mm/min. Because of the wide range of normal stresses encountered in the field, applied normal stresses were ranged between 25 and 1000 kPa. An electronically instrumented load ring measured the shear forces, and current transducers measured the corresponding horizontal and vertical displacements. Three types of non-woven geotextile (abreviated as NW), belonging to two different groups, and 2 types of woven geotextile (abreviated as W) that are readily avaible in markets, were used. In the experiments, two different gradations of sand from the Turgutlu region near the city of Izmir were used. Each soil sample was tested at two different relative densities.

### 2.1. Sand properties

Turgutlu sand was used in the study, and it was decided to work with two different gradation levels. One type, named SW in the article, is in between 0 and 5 mm gradation limits, and the other type is further sieved through $No_{20}$–$No_{60}$ sieves to get the poorly graded branch of the same soil (hereafter, named SP). The particle size distribution curves of the two sand samples and some of the basic properties of the sands are given below in Figure 1 and Table 1, respectively.

### 2.2. Geotextile properties

5 types of geotextile were used in the study (Figure 2). These types can be seen in Table 2 below. The woven geotextiles and NW1 type geotextiles are polypropylene based materials, which show high durability and high rigidity (Figure 3). The Youngs modulus is in the intermediate level. The NW2 group geotextiles are polyester based materials, which are more deformable and lithe. Also, they have the lowest tensile strength of all, and are softer and more flexible than the NW1 type non-wovens and W type woven geotextiles. NW1 have an average mechanical behaviour compared to the other two types. Woven geotextiles have the highest tensile strength, but the lowest elongation at break values, which implies the stiffer nature of the material compared to the other two groups.

From the literature survey, 5 of the possibly most important factors to have important effects on the mechanical behaviour of reinforced soils are selected and listed in Table 3.

As per ASTM D 5321 [14], both square and rectangular shear boxes could be used for finding interface shear displacement characteristics. These boxes should have a minimum dimension of greater than 300 mm, 15 times the $D_{85}$ of the coarser soil used in the test, or a minimum of 5 times the maximum opening size (in plan) of the geosynthetic tested. Most recent testing

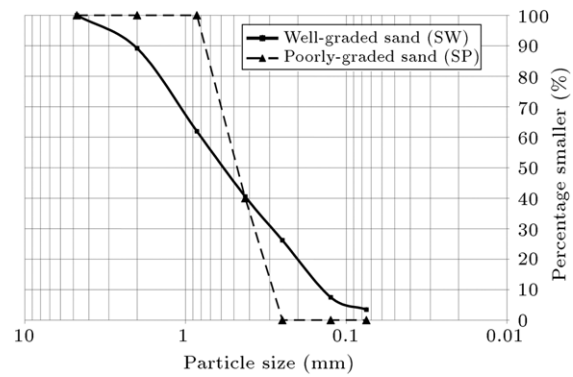


Figure 1: Particle size distribution curves of sand samples.

Table 1: Properties of sand used in experiments.

| Property | Type/value | |
|---|---|---|
| | SW | SP |
| Effective size, $D_{10}$ (mm) | 0.08 | 0.23 |
| $D_{50}$ (mm) | 0.60 | 0.47 |
| $D_{85}$ (mm) | 1.92 | 0.75 |
| Coefficient of uniformity, $C_u$ | 10.00 | 2.61 |
| Coefficient of curvature, $C_c$ | 2.18 | 1.34 |
| Soil classification (unified) | SW | SP |
| Specific gravity, $G_s$ | 2.65 | 2.65 |
| Maximum dry density, $\gamma_{max}$ (kN/m$^3$) | 17.90 | 15.80 |
| Relative density (%) | 66.70–25.00 | 63.00–25.00 |
| $e_{min}$ | 0.38 | 0.56 |
| $e_{max}$ | 0.72 | 0.86 |

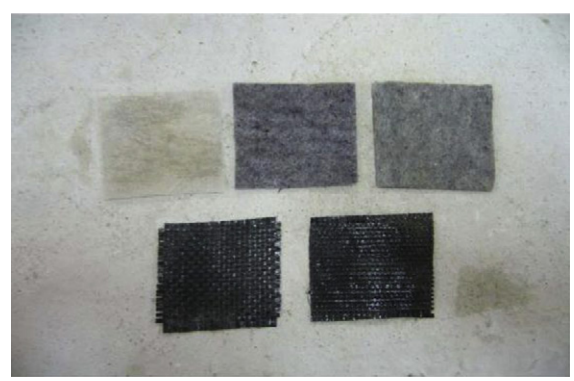

Figure 2: Different types of geotextiles used in the experiments (top from left to right: the non-woven geotextiles NW1, NW2-a, and NW2-b; bottom from left to right: the woven geotextiles, W1 and W2).

Table 2: Types of geotextile used in the study (provided from the suppliers technical brochures).

| Geotextile label | Geotextile type | Nominal mass per unit area (g/m$^2$) | Thickness (mm) | Tensile strength (N/m) | Elongation at failure (%) | Openinge size (mm) |
|---|---|---|---|---|---|---|
| NW1 | Non-woven | 150 | 0.46 | 10,300 | 52 | 0.10 |
| NW2-a | Non-woven | 250 | 2.50 | 8,000 | 50 | |
| NW2-b | Non-woven | 100 | 1.00 | 2,500 | 80 | 0.17 |
| W1 | Woven | – | | 80,000 | 8.50–13.50 | 0.12 |
| W2 | Woven | – | | 25,000 | 13–15 | 0.23 |

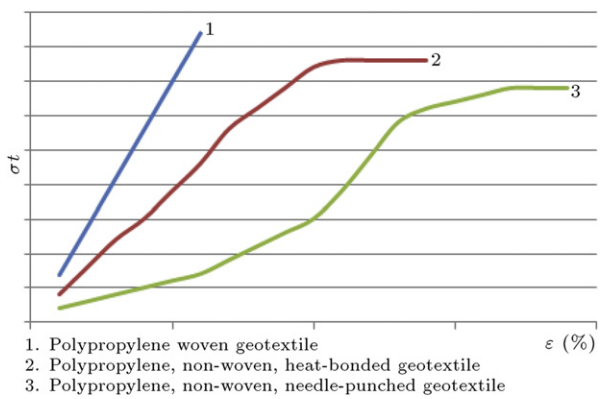


Figure 3: Mechanical behaviour of polypropylene group geotextiles.

Table 3: Experimental program.

| No | Effect to be investigated | Variables |
|---|---|---|
| 1 | Soil gradation effect | Well-graded sand<br>Uniformly-graded sand |
| 2 | Equipment effect | 60 mm ∗ 60 mm shear box<br>100 mm ∗ 100 mm shear box |
| 3 | Physical properties of geomaterials | 65% relative density<br>25% relative density |
| 4 | Confining pressure | Low $C$. pressure<br>High $C$. pressure |
| 5 | Geosynthetic properties | 5 different types |

was performed in apparatus sizes greater than the conventional direct shear apparatus, in the range of about 15–30 cm square boxes. However, it was observed by various researchers [5,10,13,15] that apparatus size does not significantly affect the friction angles for cohesionless sands.

SW and SP sands have $D_{50}$ values of 0.60 and 0.47 mm, and $D_{85}$ values of 1.92 mm and 0.75 mm, respectively. The maximum geotextile opening size is 0.23 mm. Considering the grain size of sands and geotextile opening sizes, the smaller size shear box (60 mm ∗ 60 mm) also meets the minimum equipment requirement for interface testing, after suitably modifying the box for use with geotextile specimens.

After carefully preparing the soil samples according to their desired densities and placing them in the lower box, the geotextile is mounted at the interface with the appropriate arrangements. There are some different methods for the arrangement of geotextiles in direct shear tests. Takasumi et al. [10] stated three different arrangements; the fixed shear test, partially fixed shear test and a free shear test. In this study, a freely laid geotextile sheet is further streched by fastening it from outside the boxes. Therefore, a partially fixed arrangement is most appropriate for this type. The most important issue is for the geotextile-sand composites to interact with each other without any restrictions. The geotextile specimen between the soil layers should not stretch, and also there should be no wrinkles in the specimen.

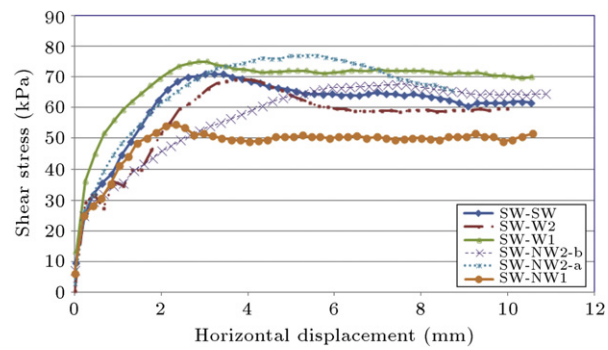


Figure 4: Stress–displacement relationships of SW sand at 65% relative density reinforced with different types of geotextile.

## 3. Results and analysis

Interface behaviour cannot be expressed by the distinct properties of each component of the system, but with an integration of each component and environmental factors. The particle size of the granular material, and the openings of the geotextiles being tested, play an important role in the final behaviour. Geotextile surface properties and mechanical characteristics affect the range of the interface zone. The dilative characteristics of granular materials under applied normal stresses are decisive characteristics of reinforced soil behaviour. An effort to explain some outcomes of the study are described in the following paragraphs.

As a first outcome of the work, consider Figure 4 below, which shows the reinforcement effects on the results. The horizontal displacement is shown via the percentage of the maximum horizontal displacement in the experiments (in the range of 5–7 mm). There was a considerable loss of shear strength seen after the peak stress, but this loss was reduced in the reinforced soils, which is a direct result of the composite enhancement effect of geotextile and sand [16]. Increasing the geotextile layers enhances the confinement effect, thus, reinforced sand becomes more ductile than unreinforced sand. Shear band development in the failure state is restricted, with geotextile inclusion in the interface area.

### 3.1. Effect of normal stress

Normal stress is a significative factor in the development of friction force. From the results, the interface friction angle initially decreases to a certain range of normal stress, and then starts to increase to a certain amount (Figure 5). The critical normal pressure range is typically between 600 and 650 kPa. The trends of the results are similar to the findings of Tan et al. [17]. The decrease in interface friction angles is attributed to the incoherency between the increase in shear stress and normal stress at the interface. The increase in normal pressure does not directly cause an increase in shear stress, because, in

REFERENCE 1



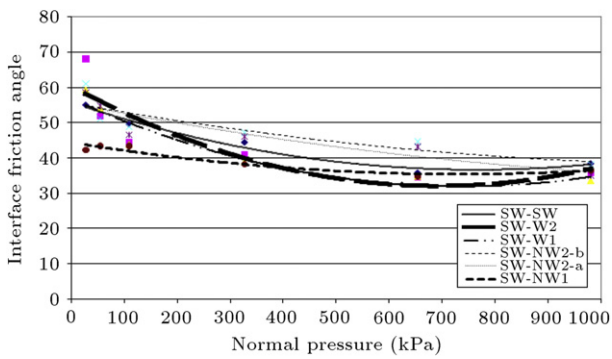


Figure 5: Influence of normal pressure on interface friction angle.

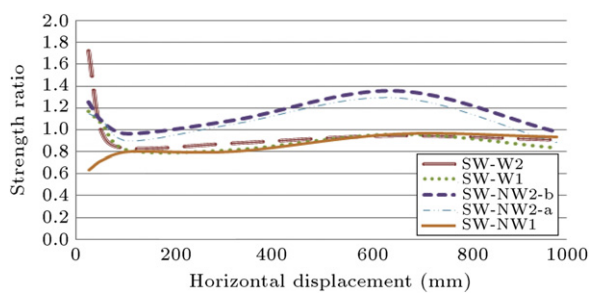


Figure 6: Strength ratio of well-graded sand (SW) at 66.7% relative density with 5 different geotextiles.

Table 4: Results of direct shear tests on reinforced SW sand.

| Interface type | Normal stress/peak shear stress (kPa) | | | Cohesion (kPa) | Interface friction angle (°) |
|---|---|---|---|---|---|
| | 27.20 | 54.50 | 109.00 | | |
| SW–SW | 39.00 | 71.10 | 128.60 | 36.00 | 36.50 |
| SW-W1 | 45.60 | 75.00 | 104.70 | 39.00 | 32.00 |
| SW-NW2-b | 49.10 | 67.50 | 124.40 | 48.00 | 38.40 |
| SW-NW2-a | 44.60 | 77.00 | 115.10 | 55.00 | 35.60 |
| SW-NW1 | 24.70 | 51.50 | 102.90 | 13.00 | 35.60 |
| SW-W2 | 67.20 | 69.20 | 106.80 | 40.00 | 33.70 |

the contact area with an increase in normal stress more and more particles become in contact with each other, resulting in a decrease of normal pressure on each contact point. After a critical pressure, this increase in particle contact comes to an end, so it becomes harder to displace each contact area.

Strength ratio is defined as the ratio of the shear strength of reinforced soil to the shear strength of unreinforced soil (Figure 6). The friction angles begin to taper off at about 500–700 kPa, whereas reinforced sand shear strength begins to increase at lower normal stresses; at nearly 100–200 kPa.

Table 4 shows peak shear stresses and corresponding normal stresses from the failure envelope, and also the cohesion values and interface friction angles determined with the best-fitted regression linear lines.

### 3.2. Effect of sample size

It is interesting to note the high cohesion values from the test results. This effect is attributed to the restraint impact of the small sized sample. In the analysis, the cohesion value should be taken as zero, and the failure line should be shifted until the cohesion value is set to zero.

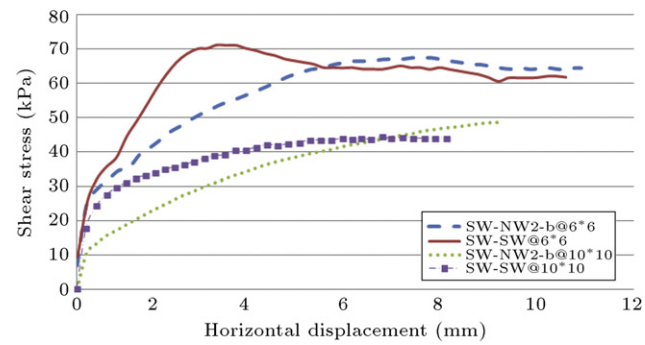


Figure 7: Stress–displacement results of the two different box sizes; $P = 49$ kPa for 10 cm $*$ 10 cm size and $P = 54.5$ kPa for 6 cm $*$ 6 cm size.

To control the results, a different set of experiments were performed with a 100 mm $*$ 100 mm sized direct shear box. The size effect on cohesion values can easily seen from Table 5.

Small sized samples show higher peak shear strength than the big sized sample (Figure 7). This type of behaviour is attributed to the confinement effect of the 60 mm $*$ 60 mm sized shear box; implicitly, high cohesion values. Similar results were found by Takasumi et al. [10] with medium dense-non-woven geotextile interface direct shear tests of 30 and 6 cm sized samples. Below 65 kPa normal pressure, the small sized sample gave higher strength values.

### 3.3. Effect of geotextile arrangement

One of the disadvantages of direct shear tests compared to other strength tests is the predetermined failure plane. Taking this fact into account, we can have an understanding of the indirect effect of geotextile inclusions by placing them above and below the failure plane. Three different types of geotextile were placed in two layers at the same distance from above and below the failure plane to have an idea of the effect of the interface zone on shearing behaviour. These different arrangements are generally used with other equipment, like the triaxial apparatus or some modified apparatus [18]. The results are given in Table 6.

The peak state could not be reached, especially under higher normal loads, in two-layered reinforced samples, whereas it was reached at about 40%–50% of the final displacement in unreinforced and one-layered reinforced samples. A two-layered reinforced sample needs more horizontal displacement at the interface to fully develop its strength, compared to one-layered reinforced and unreinforced samples (Figure 8). Also, as the confinement increases in two-layered reinforcement, the cohesion value increases substantially compared to one-layer reinforced and unreinforced samples (Figure 9).

### 3.4. Effect of relative density

The influence of soil density has been previously investigated by several researchers [19]. 65% and 25% of the relative densities of the two types of sand were tested using the direct shear apparatus. As expected, the denser the sand, the higher the interface shear strength (Figure 10). In geotextile-reinforced sand specimens, the volumetric expansion is more pronounced (Figure 11). The reason is the replaced sand particles neighbouring the geotextile inclusions. In geotextile reinforced sands, the denser sand tends to dilate more than the

## Technical Paper by A. De and T.F. Zimmie

# ESTIMATION OF DYNAMIC INTERFACIAL PROPERTIES OF GEOSYNTHETICS

**ABSTRACT:** The dynamic frictional properties of different geosynthetic interfaces play an important role in the stability analyses of various geotechnical structures that incorporate geosynthetics. The paper presents and discusses laboratory test results on eight different interfaces, formed through various combinations of three geosynthetics (a geotextile, a smooth geomembrane, and a geonet). The dynamic frictional properties were estimated using cyclic direct shear tests, shaking table tests conducted at a normal g-level of 1g as well as at high g-levels, and on a 100 g-ton geotechnical centrifuge. The centrifuge simulated high normal stress levels, commonly encountered by geosynthetics comprising base liners of landfills or base isolators for large structures. The tests revealed various important characteristics regarding the dynamic frictional properties of the geosynthetic interfaces, including a dependence of some of the interfaces on the level of normal stress and the excitation frequency. It is felt that these differences should be considered when selecting proper test methods in relation to the application for which the geosynthetic is considered. It was concluded that proper simulation of field conditions in laboratory experiments is important to obtain suitable friction angle values to be used in design.

**KEYWORDS:** Landfill liner, Geotextile, Geomembrane, Geonet, Dynamic friction angle, Cyclic shear test, Shaking table, Geotechnical centrifuge.

**AUTHORS:** A. De, Senior Staff Engineer, GeoSyntec Consultants, 1500 Newell Avenue, Suite 800, Walnut Creek, California 94596, USA, Telephone: 1/925-943-3034, Telefax: 1/925-943-2366, E-mail: anirbande@geosyntec.com; and T.F. Zimmie, Professor, Department of Civil Engineering, Rensselaer Polytechnic Institute, Troy, New York 12180, USA, Telephone: 1/518-276-6939, Telefax: 1/518-276-4833, E-mail: zimmit@rpi.edu.

**PUBLICATION:** *Geosynthetics International* is published by the Industrial Fabrics Association International, 1801 County Road B West, Roseville, Minnesota 55113-4061, USA, Telephone: 1/612-222-2508, Telefax: 1/612-631-9334. *Geosynthetics International* is registered under ISSN 1072-6349.

**DATES:** Original manuscript received 30 July 1997, revised version received 17 December 1997 and accepted 2 January 1998. Discussion open until 1 September 1998.

**REFERENCE:** De, A. and Zimmie, T.F., 1998, "Estimation of Dynamic Interfacial Properties of Geosynthetics", *Geosynthetics International*, Vol. 5, Nos. 1-2, pp. 17-39.

## 1 INTRODUCTION

The frictional properties of different geosynthetic interfaces play an important role in the stability analyses of various geotechnical structures that incorporate geosynthetics. Many of the geosynthetic surfaces in composite liner systems of modern landfills are characterized by relatively low friction angles. This causes the interfaces between such elements to be likely locations for slip movement. Recent requirements to include considerations for seismic impact in modern landfill designs have led to the need for understanding the dynamic frictional properties of these interfaces. The use of different types of geosynthetic materials for the purpose of base isolation also requires estimation of the dynamic frictional properties of the interfaces under suitable loading conditions and frequencies of excitation.

## 2 BACKGROUND

The importance of interfacial frictional properties of geosynthetics in landfill design was demonstrated by the Kettleman Hills, California landfill failure which occurred in 1988. Subsequent analyses led to extensive research into the static or monotonic frictional properties of geosynthetic interfaces (Mitchell et al. 1990a; Mitchell et al. 1990b; Byrne et al. 1992; Stark and Poeppel 1994). The most common apparatuses/methods used to estimate the static friction angles included direct shear devices (both small- and large-size), pull-out boxes, and ring shear devices. Some of the results from these studies demonstrated unique trends that were characteristic of the different testing procedures.

As a result of this extensive range of testing programs, a broad understanding of the characteristic features of different static (or monotonic) testing methods is available. Gilbert et al. (1995) have compiled a summary of the advantages and disadvantages associated with different test devices that measure interface shear strength. The devices included in the summary are the large-scale direct shear box, conventional direct shear box, torsional shear device, tilt table, and Texas double shear device.

### 2.1 Dynamic Friction Tests

Experimental research to estimate the dynamic frictional properties of geosynthetic/geosynthetic interfaces has been conducted relatively recently (Hushmand and Martin 1990; Kavazanjian et al. 1991; Yegian and Lahlaf 1992b; Pasqualini et al. 1995; Zimmie et al. 1994; Yegian and Harb 1995; De 1996). The following apparatuses were used in these studies:

- a cyclic direct shear device (Pasqualini et al. 1995; De 1996);
- a shaking table device (Yegian and Lahlaf 1992b; Hushmand and Martin 1990; Zimmie et al. 1994; De 1996); and
- a shaking table device on a geotechnical centrifuge (Hushmand and Martin 1990; Zimmie et al. 1994; De 1996).

**Table 1. Description of the geosynthetic interfaces.**

| Interface number | Geosynthetic A | Geosynthetic B |
|---|---|---|
| I | Geotextile | Smooth geomembrane |
| II | Smooth geomembrane | Geonet (transverse) |
| III | Smooth geomembrane | Geonet (longitudinal) |
| IV | Smooth geomembrane | Geonet (aligned) |
| V | Geotextile | Geonet (transverse) |
| VI | Geotextile | Geonet (longitudinal) |
| VII | Geotextile | Geonet (aligned) |
| VIII | Smooth geomembrane | Smooth geomembrane |

### 3.2.1 *Cyclic Direct Shear Device*

The direct shear apparatus used in the current study was fabricated for testing geosynthetic specimens 300 mm × 300 mm in dimension. The shear force was applied through a hydraulic actuator controlled by an MTS™ control unit. The normal force was applied by means of a pneumatic piston and compressed air. Fixed amplitudes of displacement were produced on both sides of the mean specimen position. Measurements of shear force and displacement were made continuously by means of load cells and a linear variable differential transformer (LVDT).

### 3.2.2 *Shaking Table Apparatus*

An electro-hydraulic shaking table that can accommodate specimens with dimensions up to 560 mm × 380 mm was used for the shaking table tests. Sinusoidal base motion was produced through the use of a dynamic signal analyzer. The acceleration was measured during the experiments by means of accelerometers attached to the table and to the block, and the relative displacement between the block and the table was measured using two LVDTs. Data acquisition was performed using a personal computer with commercially available software.

### 3.2.3 *Geotechnical Centrifuge*

A 100 g-ton geotechnical centrifuge was used in which high normal stresses were produced to model prototype stress conditions. The shaking table apparatus was mounted on the centrifuge platform and experiments were performed at 10g, 20g, 30g, and 40g.

## 4.3 Geotextile Over a Geonet (Interfaces V, VI, and VII)

### 4.3.1 *Cyclic Direct Shear Tests*

Figure 9 shows the plots of peak dynamic friction angle versus number of cycles for the geotextile/geonet (transverse) interface (Interface V). The dynamic friction angle of this interface appears to be strongly dependent on the normal stress. The greatest friction angle value (approximately 24°) was obtained from tests at the lowest normal stress (20.7 kPa) and the lowest friction angle (approximately 17°) corresponded to the highest normal stress (41.4 kPa). In addition, for each test, there was little variation in the friction angle with the number of loading cycles.

A likely factor for the decrease in the friction angle with the increase of normal stress may be the highly deformable nature of nonwoven geotextiles when subjected to high normal stresses. The same interface showed a nonlinear shear versus normal stress behavior during monotonic testing (De 1996), and the same trend of higher normal stresses corresponding to the lower friction angle values was observed.

Results of the cyclic tests performed on Interfaces VI and VII showed friction angles to be relatively constant with the number of loading cycles, and the dynamic friction angle did not show a strong dependence on the normal stress. In each case, the dynamic friction angle values (15° for the longitudinal orientation, and between 10 and 11° for the aligned orientation) were close to those obtained from monotonic experiments reported elsewhere (De 1996).

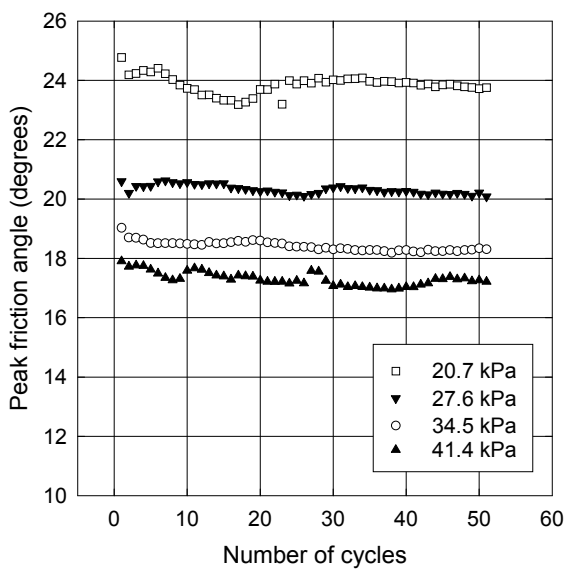


**Figure 9. Variation of the peak friction angle with the number of cycles from cyclic direct shear tests: a geotextile over a geonet (transverse) (Interface V).**

### 4.3.2 *Shaking Table Tests*

Shaking table tests on geotextile/geonet interfaces were performed using two orientations of the geonet: transverse and longitudinal. Figure 10 shows the test results for the geotextile/geonet (transverse) interface. The break point (i.e. the point at which the acceleration of the block fails to increase at the same rate as the acceleration of the table) occurs at an acceleration of 0.44g, corresponding to a dynamic friction angle of 24°. The geotextile/geonet (longitudinal) test results were similar and indicated an acceleration of 0.34g at the break point, and a dynamic friction angle of 19°.

### 4.3.3 *Shaking Table Tests Using a Geotechnical Centrifuge*

The results from the experiments performed at different acceleration levels for Interfaces V and VI are shown in Tables 5 and 6, respectively. From Table 5 it can be seen that the dynamic friction angles for Interface V at 1g, 30g, and 40g are 24°, 8°, and 7°, respectively. This shows a significant dependence on the normal stress; similar to what was observed for the cyclic direct shear test results on the same interface (Figure 9). In the case of Interface VI, the friction angle varies from 19° at 1g to approximately 10° at 40g. Centrifuge shaking table experiments were not conducted on a geotextile/geonet (aligned) interface (Interface IV).

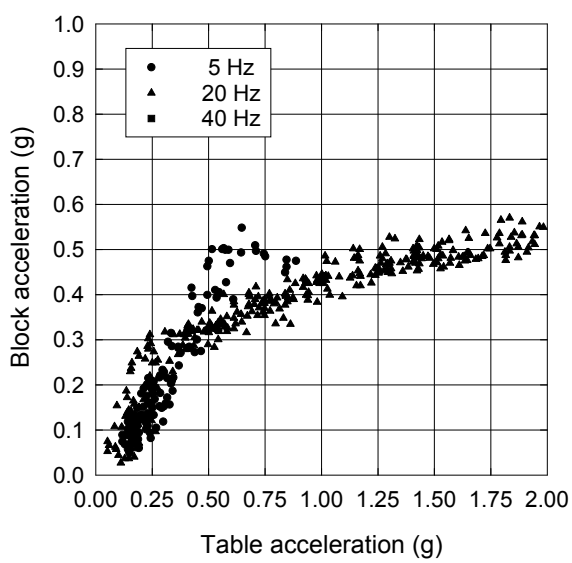


**Figure 10. Block versus table accelerations from shaking table tests: a geotextile over a geonet (transverse) (Interface V).**

**Table 5. Results from centrifuge shaking table experiments using a geotextile over a geonet (transverse) (Interface V).**

| g-level (g) | Shaking table acceleration at the inception of sliding (g) | Coefficient of dynamic friction ( = Column 2 ÷ Column 1) | Dynamic friction angle |
|---|---|---|---|
| 1 | 0.45 | 0.44 | 24° |
| 30 | 4.00 | 0.13 | 8° |
| 40 | 5.00 | **0.13** | 7° |

**Table 6. Results from centrifuge shaking table experiments using a geotextile over a geonet (longitudinal) (Interface VI).**

| g-level (g) | Shaking table acceleration at the inception of sliding (g) | Coefficient of dynamic friction ( = Column 2 ÷ Column 1) | Dynamic friction angle |
|---|---|---|---|
| 1 | 0.34 | 0.34 | 19° |
| 20 | 4.00 | 0.20 | 11° |
| 30 | 6.00 | 0.20 | 11° |
| 40 | 7.00 | 0.18 | 10° |

#### 4.3.4 *Results*

From the results shown in Section 4.3, it can be concluded that the behavior of the geotextile/geonet interfaces appears to show a dependence on the normal stress. This dependence is strong in the case of a transversely-orientated geonet (Interface V) and not as pronounced in the case of a longitudinally-orientated geonet (Interface VI).

### 4.4 Smooth Geomembrane Over a Smooth Geomembrane (Interface VIII)

#### 4.4.1 *Cyclic Direct Shear Tests*

The results of cyclic direct shear tests on Interface VIII (geomembrane/geomembrane interface) are plotted in Figure 11. The peak dynamic friction angle shows a strong tendency to increase with the number of cycles in the first 20 cycles. Following that, the rate of increase reduces, even though the increase continues to the end of the experiment which occurred after 50 cycles. There is no evidence of dependence on normal stress for these test results.

The cause for the increase in the dynamic friction angle with an increasing number of cycles is not completely understood. However, at the end of the tests, visual inspection of the specimens clearly showed surface abrasion of the geomembrane along the direction of shear displacement. It is not clear whether such abrasion was caused by the rapid movement of one layer of HDPE against another, or by a foreign object, such as dust particles present at the interface. Regardless of the cause, it is obvious that the abrasions resulted in an increase in the dynamic friction angle during cyclic loading.

REFERENCE 2



## 5 SUMMARY AND CONCLUSIONS

### 5.1 Summary of Results

The dynamic frictional behavior of eight geosynthetic interfaces have been presented in the current paper. The dynamic friction angles of the interfaces have been estimated on the basis of cyclic direct shear experiments and shaking table tests, both at 1g and high g-levels. The values of the friction angle obtained from the different experiments are listed in Table 8. For comparison, the static friction angles from tilt table and direct shear tests presented by De (1996) are also shown in Table 8.

In general, the results shown in Table 8 indicate that the initial values of static and dynamic friction angles for the geosynthetic interfaces tested are similar. However, the dynamic behavior of most interfaces is complicated by a dependence on the frequency of excitation and the number of loading cycles.

It was observed that the dynamic shear strength of geotextile/smooth geomembrane interfaces decreases slightly when subjected to repeated cycles of shear loading. This is due to the polishing effect of the geotextile on the geomembrane.

**Table 8. Average values of the peak friction angle for different geosynthetic interfaces.**

| Interface description | Static friction angle | | Dynamic friction angle | | |
|---|---|---|---|---|---|
| | Tilt table tests | Direct shear tests | Direct shear tests | Shaking table tests | |
| | | | | 1g | 10g to 40g |
| Nonwoven geotextile over smooth geomembrane | 11.8° | 12° | Decreases from 12.5 to 10.5° | 12° | 11° |
| Smooth geomembrane over geonet (transverse) | 10.1° | 11.3° | Increases from 11 to 18° (for low $\sigma$) or 14° (for high $\sigma$) | 12° | 7° |
| Smooth geomembrane over geonet (longitudinal) | 9.8° | 11.3° | Increases from 10 to 18° (for low $\sigma$) or 16.5° (for high $\sigma$) | 12° | 11° |
| Smooth geomembrane over geonet (aligned) | 8.1° | 8.1° | Increases from 9 to 18° (for both low and high $\sigma$) | --- | --- |
| Nonwoven geotextile over geonet (transverse) | 24.5° | Ranges from 22° (at low $\sigma$) to 14.5° (at high $\sigma$) | Ranges from 24° (at low $\sigma$) to 17° (at high $\sigma$) | 24° | 8° |
| Nonwoven geotextile over geonet (longitudinal) | 13.9° | Ranges from 17° (at low $\sigma$) to 14° (at high $\sigma$) | 15° | 19° | 11° |
| Nonwoven geotextile over geonet (aligned) | 11.2° | 10.5 | 11 to 10° | --- | --- |
| Smooth geomembrane over smooth geomembrane | 13.1° | 8.8° | Increases from 10.3 to 19.5° | 19° | 13° |

cerning test methods, depending on the intended functions of the interface being designed. The results of centrifuge shaking table tests on some of the interfaces indicate a dependence on normal stress and frequency. Therefore, the use of this approach should be supplemented by cyclic direct shear tests and 1g shaking table tests. Table 9 has been prepared to provide guidance to the design engineer in selecting the proper testing procedures and values for the estimation of dynamic friction angles.

## REFERENCES

Byrne, R.J., Kendall, J. and Brown, S., 1992, "Cause and Mechanism of Failure, Kettleman Hills Landfill B-19, Unit IA", *Stability and Performance of Slopes and Embankments-II*, Seed, R.B. and Boulanger, R.W., Editors, Geotechnical Special Publication No. 31, ASCE, Vol. 2, proceedings of a specialty conference held in Berkeley, California, USA, June 1992, pp. 1188-1215.

De, A., 1996, "*Study of Interfacial Friction of Landfill Geosynthetics: Static and Dynamic*", Ph.D. Thesis, Rensselaer Polytechnic Institute, Troy, New York, USA, 245 p.

Geotek, 1987, "*Direct Shear Testing of Friction Liner Material*", Report for Gundle Lining Systems, Project 21266, March 1987, 10 p.

Gilbert, R.B., Liu, C.N., Wright, S.G. and Trautwein, S.J., 1995, "A Double Shear Test Method for Measuring Interface Strength", *Proceedings of Geosynthetics '95*, IFAI, Vol. 3, Nashville, Tennessee, USA, February 1995, pp. 1017-1029.

Hushmand, B. and Martin, G.R., 1990, "*Final Report SBIR Phase I Study, Layered Soil-Synthetic Liner Base Isolation System*", Report submitted to the National Science Foundation Small Business Innovative Research Program, The Earth Technology Corporation, Long Beach, California, USA, 86 p.

Kavazanjian, E., Hushmand, B. and Martin, G.R., 1991, "Frictional Base Isolation Using a Layered Soil-Synthetic Liner System", *Proceedings of the Third U.S. Conference on Lifeline Earthquake Engineering*, Cassaro, M.A., Editor, ASCE Technical Council on Lifeline Earthquake Engineering Monograph No. 4, Los Angeles, California, USA, August 1991, pp. 1140-1151.

Ko, H-Y., 1988, "Summary of the state-of-the-art in Centrifuge Model Testing", *Centrifuges in Soil Mechanics*, Craig, W.H., James, R.G. and Schofield, A.N., Editors, Balkema, pp. 11-18.

Mitchell, J.K., Seed, R.B. and Seed. H.B., 1990a, "Kettleman Hills Waste Landfill Slope Failure. I: Liner-System Properties," *Journal of Geotechnical Engineering*, Vol. 116, No. 4. pp. 647-668.

Mitchell, J.K., Seed, R.B. and Seed H.B., 1990b, "Stability Considerations in the Design and Construction of Lined Waste Depositories", *Geotechnics of Waste Fills - Theory and Practice*, ASTM Special Technical Publication 1070, Landva, A. and Knowles, G.D., Editors, proceedings of a symposium held in Pittsburgh, Pennsylvania, USA, September 1989, pp. 209-224.

Pasqualini, E., Sani, D. and Roccato, M., 1995, "Factors Influencing Geomembrane Interface Friction", *Green '93*, Sarsby, R.W., Editor, Balkema, proceedings of a conference held in Bolton, United Kingdom, June 1993, pp. 349-356.

Schofield, A.N., 1980, "Twentieth Rankine Lecture: Cambridge Geotechnical Centrifuge Operations", *Geotechnique*, Vol. 20, No. 3, pp. 227-268.

Stark, T.D. and Poeppel, A.R., 1994, "Landfill Liner Interface Strengths from Torsional-Ring-Shear Tests", *Journal of Geotechnical Engineering*, Vol. 120, No. 3, pp. 597-615.

Von Pein, R.T. and Lewis, S.P., 1991, "Composite Lining System Design Issues", *Geotextiles and Geomembranes*, Vol. 10, Nos. 5-6, pp. 125-131.

Yegian, M.K. and Harb, J.N., 1995, "Slip Displacements of Geosynthetic Systems Under Dynamic Excitation", *Earthquake Design and Performance of Solid Waste Landfills*, Yegian, M.K. and Finn, W.D.L., Editors, Geotechnical Special Publication No. 54, ASCE, proceedings of a specialty conference held in San Diego, California, USA, October 1995, pp. 212-236.

Yegian, M.K. and Lahlaf, A.M., 1992a, "Discussion of 'Kettleman Hills Waste Landfill Slope Failure. I: Liner-System Properties' by Mitchell, J.K., Seed, R.B. and Seed. H.B.", *Journal of Geotechnical Engineering*, Vol. 118, No. 4, pp. 643-645.

Yegian, M.K. and Lahlaf, A.M., 1992b, "Dynamic Interface Shear Strength Properties of Geomembranes and Geotextiles", *Journal of Geotechnical Engineering*, Vol. 118, No. 5, pp. 760-778.

Zimmie, T.F., De, A. and Mahmud, M.B., 1994, "Centrifuge Modelling to Study Dynamic Friction at Geosynthetic Interfaces", *Proceedings of the Fifth International Conference on Geotextiles, Geomembranes and Related Products*, Vol. 1, Singapore, September 1994, pp. 415-418.

REFERENCE 3

A Report
on

# COMPARISON OF PVC and HDPE GEOMEMBRANES (INTERFACE FRICTION PERFORMANCE)

for

PVC GEOMEMBRANE INSTITUTE.

Dr.Shobha K.Bhatia
Gautam Kasturi
Dept. of Civil and Environmental Engineering
SYRACUSE UNIVERSITY

## 1.0 INTRODUCTION

Modem solid-waste landfills and hazardous landfills in the USA are required to have a low hydraulic conductivity liner and drainage system, consisting of geosynthetic materials (geomembranes, geotextiles, geonets and geocomposites) and compacted clay. A cross-section of a typical modem landfill, as shown in Figure 1.1, consists of several layers of soils and geosynthetic products. The stability of these 'slopes' is controlled by the shear strength of the various interfaces in such a composite liner. Critical interfaces include soil vs. geomembrane, soil vs. geotextile, geomembrane vs. geotextile and geomembrane vs. geonet. The strength of each of these interfaces has to be determined after careful, site-specific material testing (Koerner, 1994). The experience and confidence gained from these tests on different materials and soils is valuable to designers. Such data give the basis for better judgment in design. The importance of the evaluation of interface strength has been illustrated by the slope stability failure in Phase 1A of the construction of the Kettleman Landfill in California (Mitchell et al., 1990).

Geomembranes are critical components of modem landfill design, performing important functions moisture barriers in the containment system. Today, a variety of geomembranes are in use in current practice. The basic difference between them is the material and/or method of manufacture. The most commonly-used material types are (PVC) Poly Vinyl Chloride and (HDPE) High Density Poly-Ethylene. Based on a 1992 estimated total of 648 million sq. feet of geomembrane sales, HDPE accounts for 259 million sq. feet or 40 % of sales , while PVC accounts for 162 million sq. feet or 25 % of sales(Koerner, 1994). Very Low Density Poly-Ethylene (VLDPE), a Polyethylene product, which is more flexible than HDPE, accounts for 65 million sq. ft or 10 % of sales .

Geomembrane interface frictional failure has been identified as the cause of numerous geosynthetic-lined slope failures. As a result, the interface frictional strength of any geomembrane interface has to be determined with utmost care. It is recommended that wherever possible, the interface frictional strength for a geomembrane-soil combination be determined experimentally, without resorting to use of generalized values for similar soils from published data (Koerner, 1994). Direct shear, pullout and ring shear tests have been performed extensively, mainly on soil-geomembrane interfaces, to characterize their strengths (Koerner et al., 1986; Seed et al., 1988; O'Rourke et al., 1990; Takasumi et al, 1991; Stark and Poeppel, 1994)

There have been a limited number of testing programs that have attempted to draw a general comparison between HDPE and PVC geomembranes. O'Rourke (1990) reported that the higher the stiffness or hardness of the geomembrane, like HDPE, the lower the friction angle, as compared to a flexible membrane, like PVC. Martin et al. (1984) tested geotextile vs. geomembrane interface friction using a very soft, flexible geomembrane like Ethylene Propylene Diene Monomer (EPDM), a medium stiffness PVC geomembrane and a tough geomembrane like HDPE. They also concluded that the softer geomembranes, have greater friction angles than the tougher geomembranes.

**Table 2.1 Properties of Geomembranes used in the Testing Program**

| GEOMEMBRANE TYPE | *SMOOTH PVC[1]* | *TEXTURED PVC[2]* | *FILE-FINISH PVC[3]* | *SMOOTH HDPE[4]* | *TEXTURED HDPE[5]* |
|---|---|---|---|---|---|
| MANUFACTURER | Oxychem | **OxyChem** | **C.G.T. Ltd.** * | **GSE**** | **GSE** |
| TRADE NAME | **Oxyflex** | **OxyGrip** | **Taffeta** | **GSEHD** | **GSEHDT** |
| GAUGE ( mils ) | 30 | 30 | 30 | 60 | 60 |

* Canadian General Towers
** Gundle / SLT Environmental ( Inc. ) Company
1. Smooth PVC : Smooth, flexible PVC geomembrane
2. Textured PVC : PVC geomembrane, with extrusions of 4 - 6 mils on the surface, giving the rough texture. The textured surface was used as the interface
3. File-Finish PVC : Square grid etched onto one surface, with smooth PVC on the other surface. The surface with the file-finish was used as the interface.
4. Smooth HDPE : Smooth, tough, inflexible HDPE geomembrane
5. Textured HDPE : Co-extruded textured surface on one side and smooth HDPE on the other surface. The textured surface was used in the surface.

2.1.2 Soil

A typical landfill consists of soil-geomembrane interfaces involving a variety of soils. Most commonly, sand as a drainage layer and clay as a moisture barrier are used. However, when locally available soils are the only option, sandy loam and silty clay are used as substitutes. Hence, these soils were also included in this study. Figure 2.1 gives the grain size distribution of the soils.

*2.1.2.1 Sand*

Sand-Geomembrane interfaces are common at the boundary of a drainage layer and the next layer of moisture barrier. Testing for this interface was performed using sand with the following properties :

Grain size distribution :

$D_{10}$ - 0.15 mm $D_{50}$ - 0.29 mm $D_{90}$ - 0.51 mm
$C_u$ - 2.13 $C_c$ - 0.919
Internal Friction : Angle of Internal Friction, from a Direct Shear Test = 32.3"

This sand can be described as uniform, fine sand. It was mixed with just enough water to simulate the average field wetness conditions (approximately 10%).

### 2.1.2.2 *Sandy Loam*

In many situations, the soils most suitable for a landfill may not be available on location. In such cases, liners are constructed with the available soil. One of the common soils found at sites is sandy loam. In such situations, sandy loam is used as an alternative to sands in the landfill. The soil used for testing in this program can be described as well graded sandy loam. In this soil, there was a significant amount of organic matter, including plant root fibers and remains of insects. The natural water content of the soil was 41.8 % . Testing was done at the same water content.

The requirements of a material to be used as drainage material in a waste containment system are as follows ( USEPA, 1989 ) :

- Hydraulic conductivity must be greater than $10^{-2}$ cm / s ;
- Rounded to sub-rounded material, to avoid damage to the adjacent geosynthetics ;
- Well graded material ; and
- Maximum particle size of 3 / 8 inch ( 9.5 mm ) .

The properties of the sandy loam used in this study were :

<u>Grain size distribution characteristics</u> :

| | | |
|---|---|---|
| $D_{10}$ - 0.10 mm | $D_{50}$ - 0.53 mm | $D_{90}$ - 4.2 mm |
| $C_u$ - 9.0 | $C_c$ - 0.69 | |

Based on the USEPA requirements above for a drainage material, the sandy loam tested satisfies the requirements for use as a drainage material. The hydraulic conductivity requirement needs to be verified, but it is strongly believed that it will be complied, based on its grain size distribution.

### 2.1.2.3 *Silty Clay*

Locally available soil is generally preferred for the compacted clay layer in a landfill liner. In such cases, the criteria for selecting the soil are(Daniel, 1993) :

- % dry weight passing the #200 sieve >= 39 % - 50 %
- % dry weight retained on the # 4 sieve <= 20 % - 50 %
- PI (ASTM D 4318) >= 7 % - 10%
- Maximum grain size : 25 mm - 50 mm

<u>Grain size distribution characteristics</u> :

| | | |
|---|---|---|
| $D_{10}$ - < 0.075 mm | $D_{50}$ - 0.12 mm | $D_{90}$ - 4.3 mm |
| $C_u$ - 23.17 | $C_c$ - 1.03 | |

Similarly, the stress measured was that between the geomembrane and the soil as well, because those were the only two materials in contact as the top box moved relative to the bottom box.

The high value of $R^2$ for the graph of the failure envelope ( Figure 3.2(b) ) indicates that the $\phi$ value for this interface was not affected by the confining stress level, although it may be different for much lower confining stresses ( less than 10 kPa ).

### 3.2 Sand vs. the Other Geomembranes

The relationships for fine sand vs. smooth HDPE interface are shown in Figures 3.3 (a) and (b). The same relationships, stress vs. displacement and interface friction angle, for sand vs. the rest of the geomembranes in the testing program, are given in Appendix A. Stretching was observed in the File-finish PVC interface at higher normal stresses (greater than 100 kPa). Strain softening behaviour was noticed with HDPE. Textured HDPE exhibited peak values at higher displacements (about 35 mm). However, textured PVC did not reveal a clear trend in its stretching.

### 3.3 Influence of Soil Type

The study of the variation of interface friction values of the same geomembranes with soil type shows considerable difference in the stress-strain behaviour as well as friction angle values. Figures 3.4 and 3.5 give relationships of smooth PVC interfaces against sandy loam and silty clay respectively. Figures showing these relationships for interfaces with other geomembranes are given in Appendix B (Sandy Loam) and Appendix D (Silty Clay).

### 3.4 Geomembrane vs. Geotextile

The relationships for the smooth PVC vs. geotextile interface are shown in Figure 3.6. Interface friction values of the other geotextile-geomembrane interfaces are given in Appendix D.

## 4.0 SUMMARY OF RESULTS

The results of the testing program are summarized in Tables 4.1 and 4.2. The interface friction angles based on stress obtained at about 10 % strain (25.4 mm) from the stress displacement curves are given in Table 4.1. Table 4.2 gives the interface friction angles based on the peak stress obtained from the stress-displacement graphs. In the case of HDPE and textured-HDPE membranes, the stress-displacement response of the interface is such that after reaching peak stress, further shearing to a larger strain causes stabilization of the stress (remains constant ; see Figure 3.3). Hence, the shear stress at 10% strain for the rigid membranes (HDPE and HDT) is less than at the peak. However, for the flexible membranes (PVCs), due to their stretching during the tests, the strength at higher strain is greater than at lower strain (see Figure 3.4). This was observed with all PVC interfaces with all the other interface materials except with fine sand.

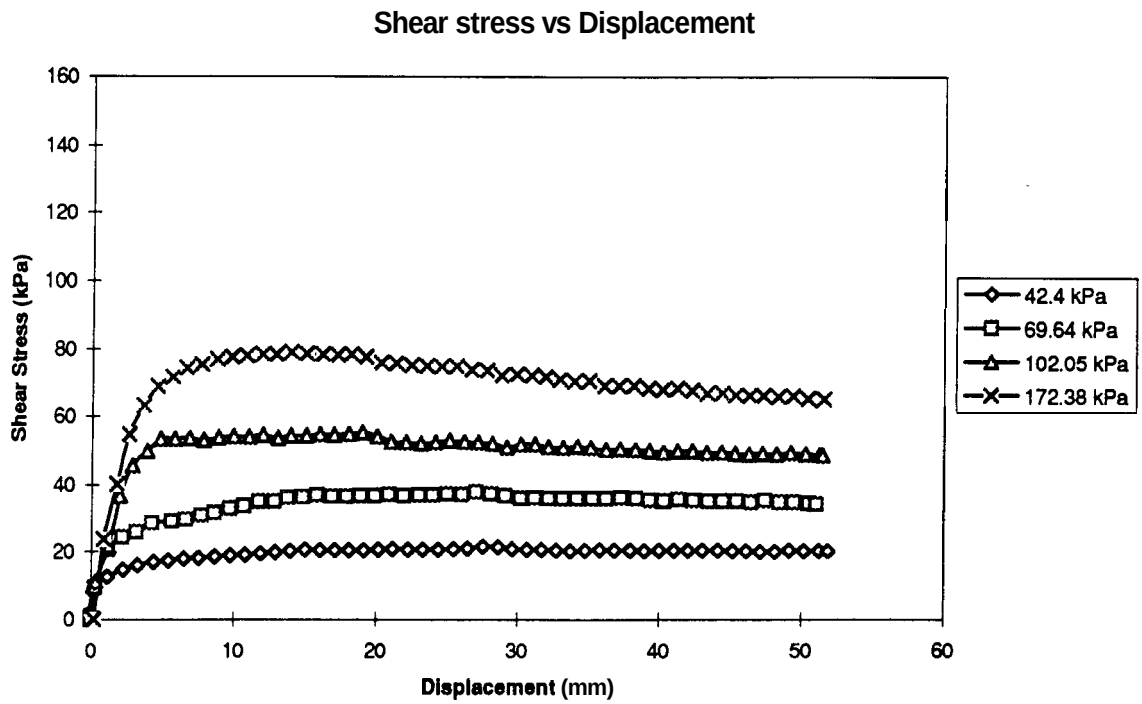


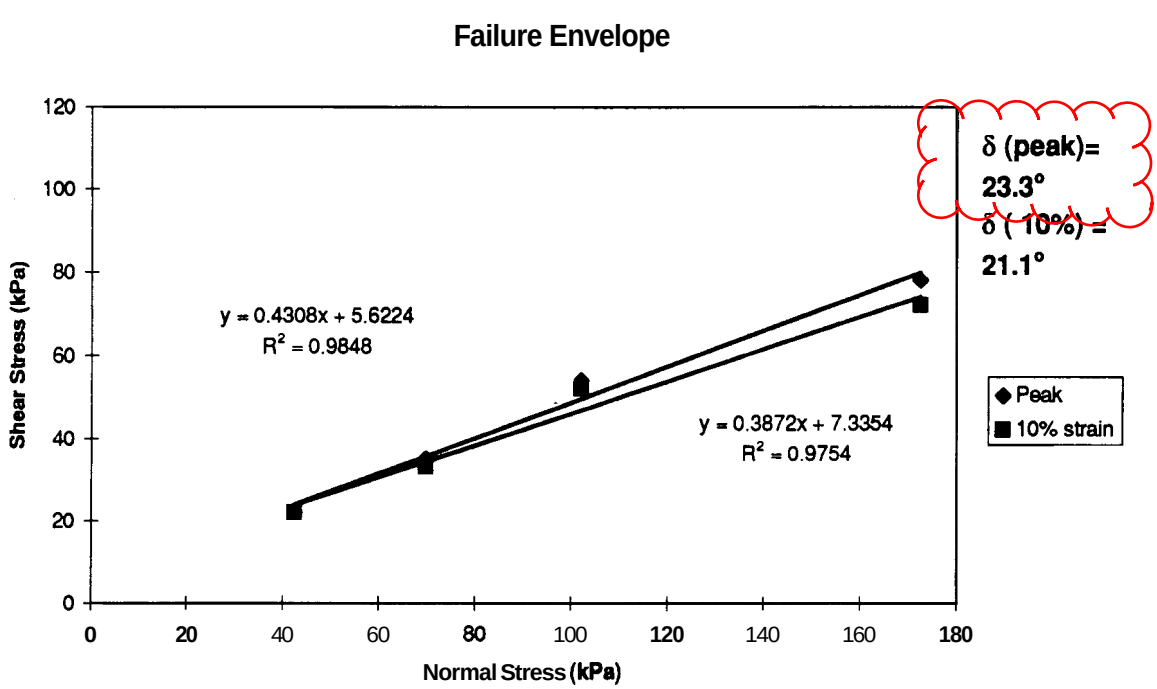


Figure 3.3 Fine Sand vs Smooth HDPE a) Shear vs Displacement b) Friction Angle

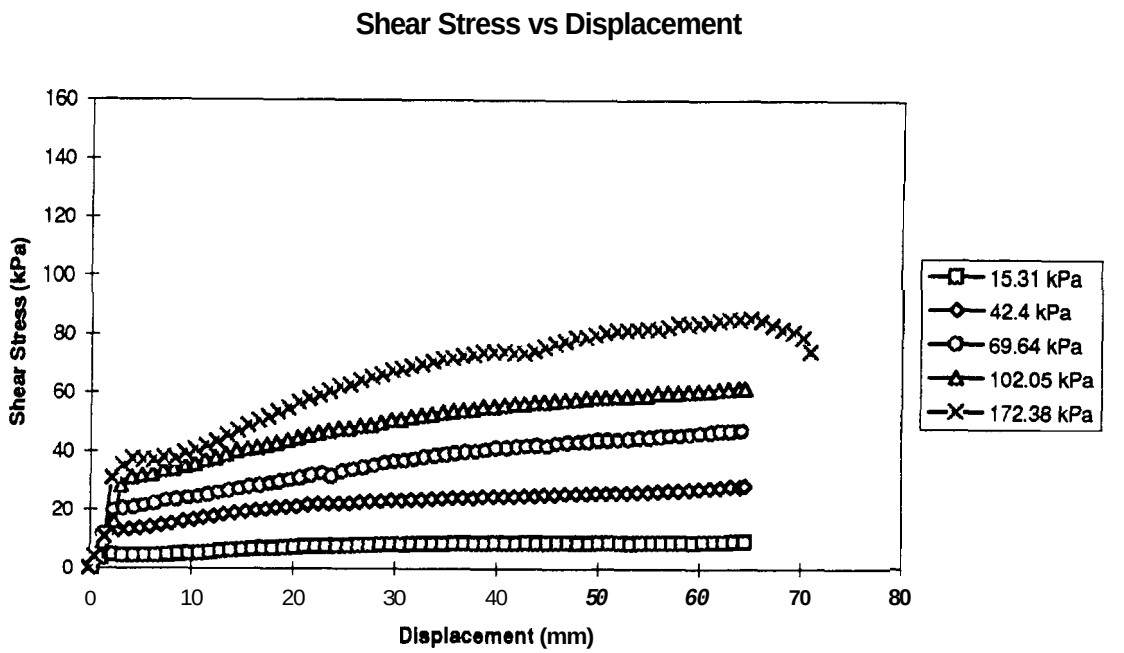


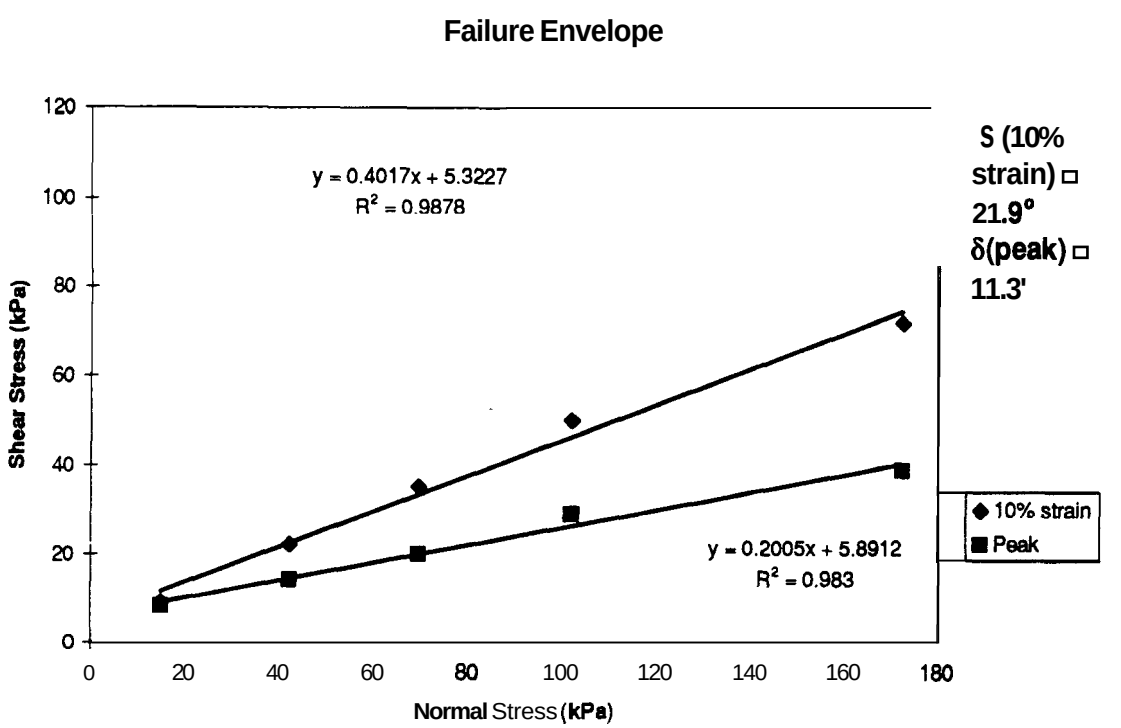


Figure 3.6 Non-Wovemn Geotextile vs. Smooth PVC a)Stress vs. Displacement b) Friction Angle

For this reason, the friction angle for the interfaces were calculated at both the peak stress and the stress at 10 % strain. It can be readily seen, comparing Tables 4.1 and 4.2, that the interface angle for PVC membranes at initial peak (yield stress for the interface) is much lower than at higher strain. However, the yield point of the interface does not represent a failure condition. This is because further shearing causes an increase in strength and not a decrease, whereas further shearing in HDPE causes reduced strength. Therefore, under field conditions, if the PVC membranes are stressed beyond the yield stress for the interface, the material stretches under the load without any loss of strength or material damage.

**Table 4.1 Interface Friction Angle values ( degree )obtained for various interfaces tested ( at 10 % strain )**

| | Fine Sand | Sandy Loam | Silty Clay | Non-woven Geotextile |
|---|---|---|---|---|
| 30 mil Smooth PVC ( at 10 % strain ) | 34.7 | 26.4 | 20.8 | 21.9 |
| 30 mil textured PVC ( at 10 % strain ) | 35.3 | 21.1 | 26.4 | 19.6 |
| 30 mil File-finish PVC ( at 10 % strain ) | 30.9 | 28.1 | 26.0 | 17.3 |
| 60 mil Smooth HDPE ( at 10 % strain ) | 21.1 | 18.2 | 17.0 | 14.2 |
| 60 mil Textured HDPE ( at 10 % strain ) | 36.6 | 33.8 | 41.8 | 17.4 |

**Table 4.2 Interface Friction Angle values ( degree )obtained for various interfaces tested ( at Peak Stress )**

| | Fine Sand | Sandy Loam | Silty Clay | Non-woven Geotextile |
|---|---|---|---|---|
| 30 mil Smooth PVC ( Peak stress ) | 34.7 | 26.4 | 21.5 | 11.3 |
| 30 mil textured PVC ( Peak stress ) | 35.3 | 19.9 | 22.9 | 13.2 |
| 30 mil File-finish PVC ( Peak stress ) | 30.9 | 28.1 | 27.7 | 11.4 |
| 60 mil Smooth HDPE (Peak stress ) | 23.6 | 25.2 | 25.8 | 15.1 |
| 60 mil Textured HDPE ( Peak stress ) | 36.6 | 33.8 | 41.8 | 17.4 |

REFERENCE 4

# WASTE TECH '94

# LANDFILL TECHNOLOGY

## JANUARY 13-14, 1994

## THE OMNI AT CHARLESTON PLACE HOTEL
## CHARLESTON, SOUTH CAROLINA

*Sponsored by the National Solid Wastes Management Association*
*1730 Rhode Island Avenue, NW, Suite 1000*
*Washington, D.C. 20036*
*202/659-4613*

Figure 3. Conformance Test Results of Interface strength Properties.

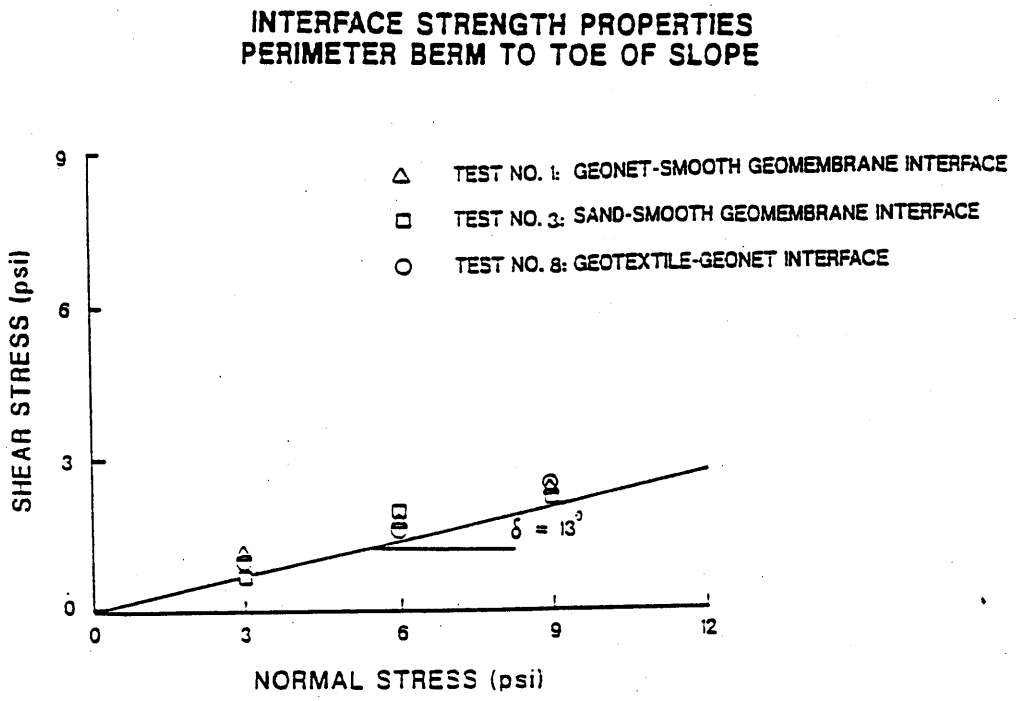


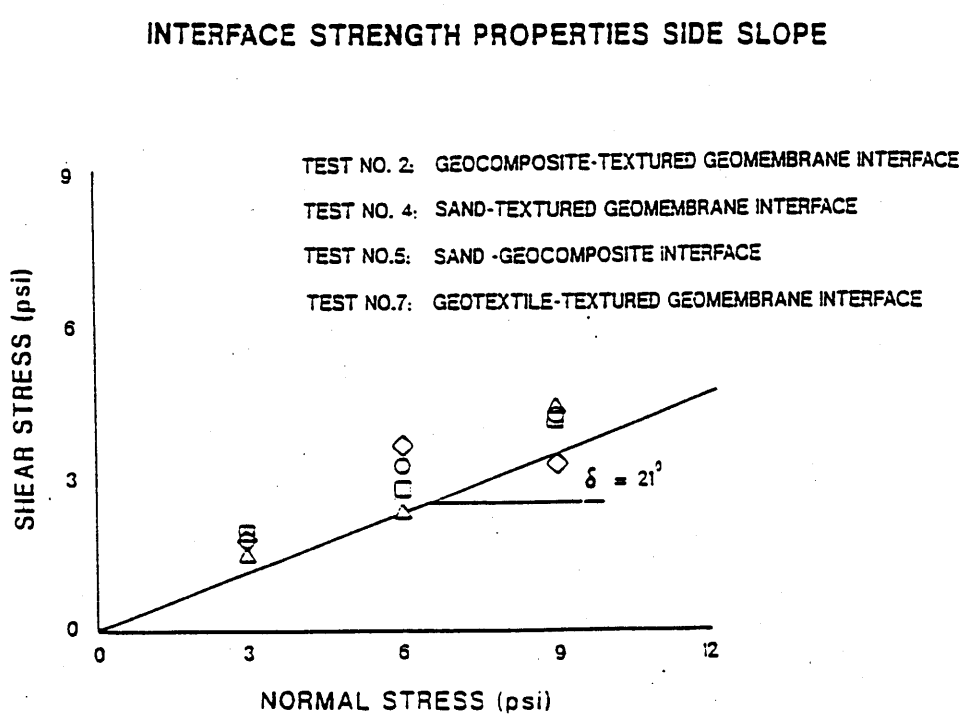

Table I. Summary of Interface Strength Parameters Used in Slope Stability Evaluation.

| Interface Description | Interface Friction Angle (degrees) | Adhesion (psf) |
|---|---|---|
| Geonet/80-mil Textured HDPE Liner | 8 | 0 |
| Geonet/80-mil Smooth HDPE Liner | 9 | 0 |
| Concrete Sand/80-mil Textured HDPE Liner | 21 | 0 |
| Concrete Sand/Geocomposite Drainage Net | 21 | 0 |

Waste Shear Strength Properties

A wide range of shear strength values for MSW materials have been reported in engineering literature. Since no waste strength properties have been measured at the site, a parametric study using a range of shear strength values (expressed in the form of internal friction angles) was conducted to evaluate the effects of waste shear strengths on the safety factor. The results of the parametric study is summarized in Table II.

It should be noted that there is observable change in the calculated safety factor when adhesion within waste is included in the analysis. Since there is no site-specific value available and adhesion within waste may not be realistically obtainable, no adhesion was used in the evaluation.

# INTERFACE FRICTION TEST RESULTS
## ASTM D 5321

geotechnics
INTEGRITY IN TESTING

CLIENT : King Construction Services, Inc.
CLIENT PROJECT : Horry County East Hill Closure
PROJECT NO. : L14061-01
LAB I. D. NO.: Skaps TN 300-2-6 Geocomposite (L14061-01-02)
Agru 40 mil LLDPE Microspike, Roll # 343519-11 (L14061-01-01)

INTERFACE : **Geocomposite**
**vs. 40 mil LLDPE Microspike (Bottom/Shiny Side)**

| | PEAK SHEAR | RESIDUAL SHEAR |
|---|---|---|
| FRICTION ANGLE (deg) : | Φ = 32.1 | Φ = 15.0 |
| COEFFICIENT OF FRICTION : | = 0.628 | = 0.269 |
| ADHESION [Calculated] (psf): | a = 19 | a = 42 |

NOTES:
1.) The interface was loaded, inundated with water and seated for 1 hour prior to shearing.
2.) The peak friction angle was calculated using linear regression on the three data points.
3.) The residual friction angle was calculated using linear regression on the end of test values.

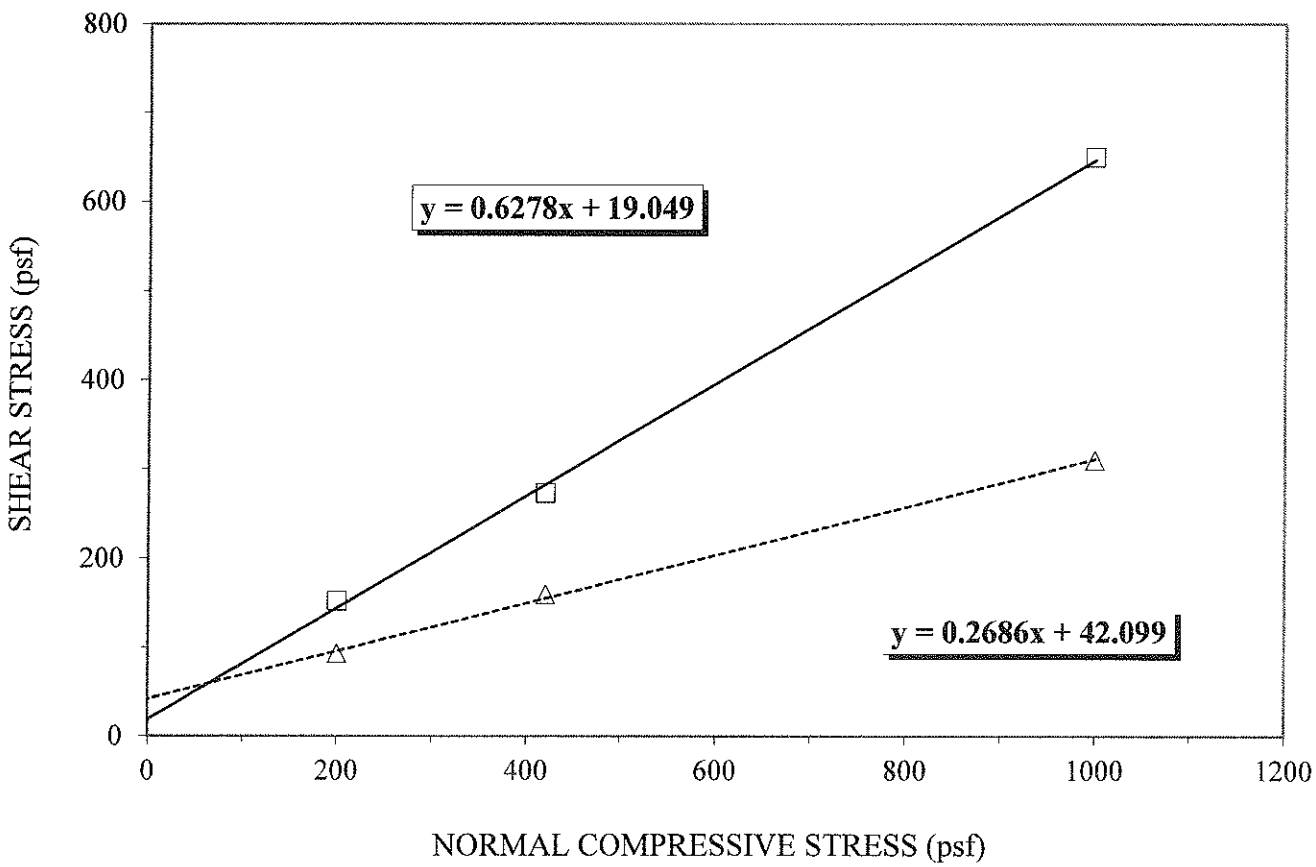


□PEAK SHEAR DATA △RESIDUAL SHEAR DATA



APPROVED BY : DATE : 6-10-14



544 Braddock Avenue • East Pittsburgh, PA 15112 • 412-823-7600 • FAX 412-823-8999 • www.geotechnics.net

# INTERFACE FRICTION TEST RESULTS
## ASTM D 5321

geotechnics
INTEGRITY IN TESTING

CLIENT : King Construction Services, Inc.
CLIENT PROJECT : Horry County East Hill Closure
PROJECT NO. : L14061-01
LAB I. D. NO.: Skaps TN 300-2-6 Geocomposite (L14061-01-02)
Agru 40 mil LLDPE Microspike, Roll # 343519-11 (L14061-01-01)

INTERFACE : **Geocomposite**
**vs. 40 mil LLDPE Microspike (Bottom/Shiny Side)**

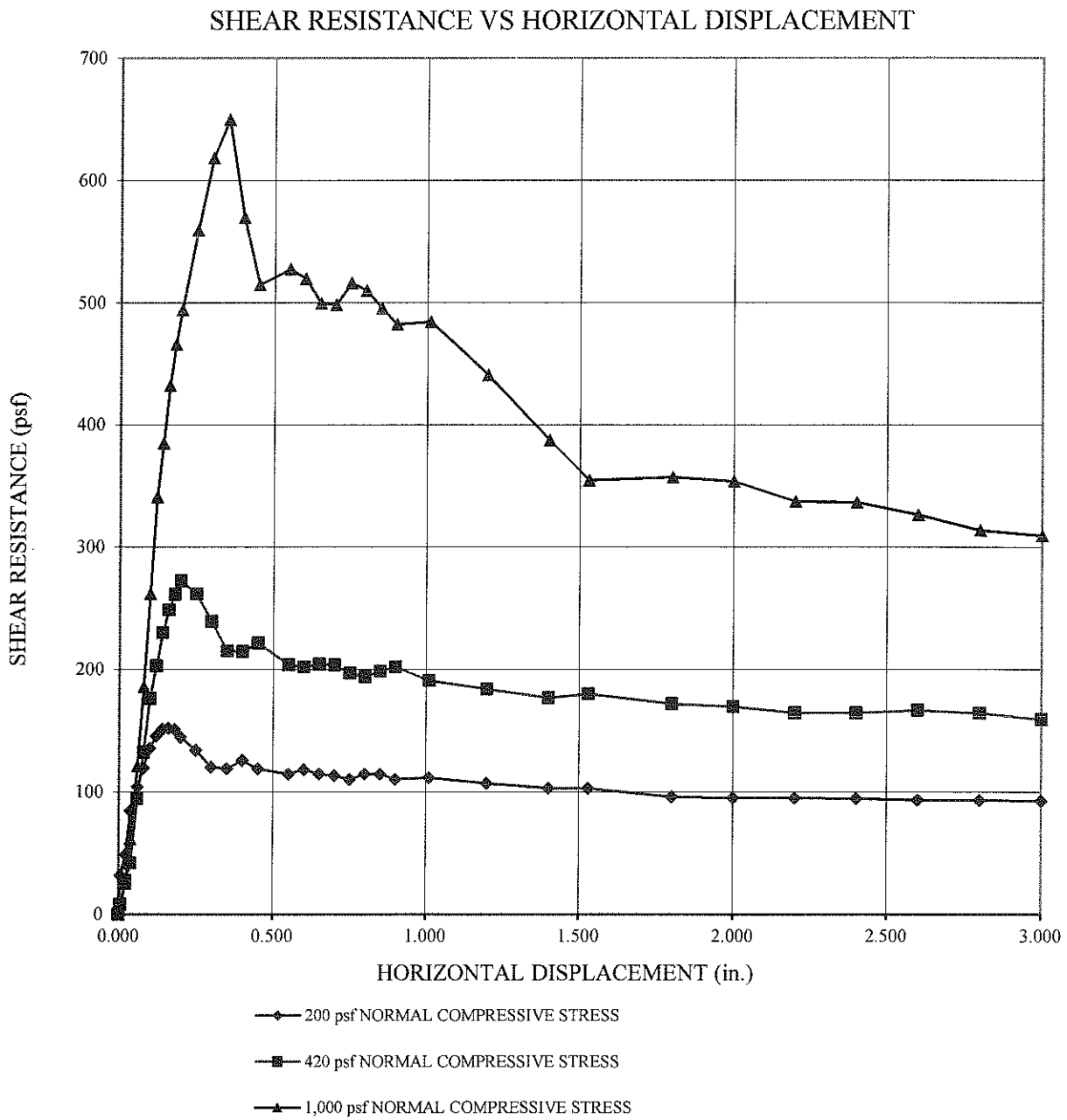




APPROVED BY : DATE : 6-10-14

\\geoserver\Data Drive\Ryan\Finished Reports\L14\061\01\[L14061-01 INT 2.xls]3 Points L14061-01 6/10/2014

544 Braddock Avenue • East Pittsburgh, PA 15112 • 412-823-7600 • FAX 412-823-8999 • www.geotechnics.net

# INTERFACE FRICTION TEST RESULTS
## ASTM D 5321

geotechnics
INTEGRITY IN TESTING

CLIENT : King Construction Services, Inc.
CLIENT PROJECT : Horry County East Hill Closure
PROJECT NO. : L14061-01
LAB I. D. NO.S: Skaps TN 300-2-6 Geocomposite (L14061-01-02)
Agru 40 mil LLDPE Microspike, Roll # 343519-11 (L14061-01-01)

INTERFACE : **Geocomposite**
**vs. 40 mil LLDPE Microspike (Bottom/Shiny Side)**

STRAIN RATE ( in / min ) : 0.20 DIRECT SHEAR UNIT: LNL
PLACEMENT CONDITION: Inundated NORMAL LOAD: Platen Weight

| | | | | | | | | |
|---|---|---|---|---|---|---|---|---|
| NORMAL LOAD (psf) | | 200 | NORMAL LOAD (psf) | | 420 | NORMAL LOAD (psf) | | 1000 |
| PEAK SHEAR STRESS (psf) | | 152 | PEAK SHEAR STRESS (psf) | | 272 | PEAK SHEAR STRESS (psf) | | 650 |
| PEAK SECANT ANGLE (deg) | | 37.3 | PEAK SECANT ANGLE (deg) | | 33.0 | PEAK SECANT ANGLE (deg) | | 33.0 |
| RESIDUAL SHEAR (psf) | | 93 | RESIDUAL SHEAR (psf) | | 159 | RESIDUAL SHEAR (psf) | | 310 |
| RESID. SECANT ANGLE (deg) | | 24.9 | RESID. SECANT ANGLE (deg) | | 20.8 | RESID. SECANT ANGLE (deg) | | 17.2 |
| ASPERITY | | 30 | ASPERITY | | 31 | ASPERITY | | 31 |
| HORIZONTAL | | | HORIZONTAL | | | HORIZONTAL | | |
| DISPLACE. (in.) | SHEAR FORCE (lbs) | STRESS (psf) | DISPLACE. (in.) | SHEAR FORCE (lbs) | STRESS (psf) | DISPLACE. (in.) | SHEAR FORCE (lbs) | STRESS (psf) |
| 0.000 | 0 | 0 | 0.000 | 0 | 0 | 0.000 | 0 | 0 |
| 0.005 | 32 | 32 | 0.005 | 8 | 8 | 0.005 | 4 | 4 |
| 0.023 | 49 | 49 | 0.023 | 28 | 28 | 0.023 | 25 | 25 |
| 0.038 | 85 | 85 | 0.038 | 42 | 42 | 0.038 | 62 | 62 |
| 0.060 | 104 | 104 | 0.060 | 95 | 95 | 0.060 | 121 | 121 |
| 0.080 | 120 | 120 | 0.080 | 133 | 133 | 0.080 | 186 | 186 |
| 0.100 | 136 | 136 | 0.100 | 176 | 176 | 0.100 | 262 | 262 |
| 0.120 | 146 | 146 | 0.120 | 203 | 203 | 0.120 | 341 | 341 |
| 0.140 | 151 | 151 | 0.140 | 230 | 230 | 0.140 | 385 | 385 |
| 0.160 | 152 | 152 | 0.160 | 249 | 249 | 0.160 | 432 | 432 |
| 0.180 | 151 | 151 | 0.180 | 262 | 262 | 0.180 | 466 | 466 |
| 0.200 | 145 | 145 | 0.200 | 272 | 272 | 0.200 | 494 | 494 |
| 0.250 | 134 | 134 | 0.250 | 262 | 262 | 0.250 | 559 | 559 |
| 0.300 | 120 | 120 | 0.300 | 239 | 239 | 0.300 | 618 | 618 |
| 0.350 | 119 | 119 | 0.350 | 215 | 215 | 0.350 | 650 | 650 |
| 0.400 | 126 | 126 | 0.400 | 215 | 215 | 0.400 | 570 | 570 |
| 0.450 | 119 | 119 | 0.450 | 222 | 222 | 0.450 | 515 | 515 |
| 0.550 | 115 | 115 | 0.550 | 204 | 204 | 0.550 | 528 | 528 |
| 0.600 | 118 | 118 | 0.600 | 202 | 202 | 0.600 | 520 | 520 |
| 0.650 | 115 | 115 | 0.650 | 204 | 204 | 0.650 | 500 | 500 |
| 0.700 | 114 | 114 | 0.700 | 203 | 203 | 0.700 | 499 | 499 |
| 0.750 | 110 | 110 | 0.750 | 197 | 197 | 0.750 | 516 | 516 |
| 0.800 | 115 | 115 | 0.800 | 194 | 194 | 0.800 | 510 | 510 |
| 0.850 | 115 | 115 | 0.850 | 199 | 199 | 0.850 | 495 | 495 |
| 0.900 | 111 | 111 | 0.900 | 202 | 202 | 0.900 | 482 | 482 |
| 1.010 | 112 | 112 | 1.010 | 191 | 191 | 1.010 | 484 | 484 |
| 1.200 | 107 | 107 | 1.200 | 184 | 184 | 1.200 | 441 | 441 |
| 1.400 | 103 | 103 | 1.400 | 177 | 177 | 1.400 | 387 | 387 |
| 1.530 | 103 | 103 | 1.530 | 180 | 180 | 1.530 | 354 | 354 |
| 1.800 | 96 | 96 | 1.800 | 172 | 172 | 1.800 | 357 | 357 |
| 2.000 | 95 | 95 | 2.000 | 170 | 170 | 2.000 | 354 | 354 |
| 2.200 | 95 | 95 | 2.200 | 165 | 165 | 2.200 | 337 | 337 |
| 2.400 | 95 | 95 | 2.400 | 165 | 165 | 2.400 | 336 | 336 |
| 2.600 | 93 | 93 | 2.600 | 166 | 166 | 2.600 | 326 | 326 |
| 2.800 | 93 | 93 | 2.800 | 164 | 164 | 2.800 | 314 | 314 |
| 3.000 | 93 | 93 | 3.000 | 159 | 159 | 3.000 | 310 | 310 |

 APPROVED BY : DATE : 6-10-14



544 Braddock Avenue • East Pittsburgh, PA 15112 • 412-823-7600 • FAX 412-823-8999 • www.geotechnics.net

# Internal and Interface Shear Strength of Geosynthetic Clay Liners

J.G. ZORNBERG
*The University of Texas at Austin, Austin, TX USA*

J.S. McCARTNEY
*University of Colorado at Boulder, Boulder CO USA*

ABSTRACT: This chapter provides the basic concepts behind geosynthetic clay liner (GCL) internal and interface shear strength values obtained from laboratory testing. Different aspects of the standard testing equipment and methods are discussed, focusing on the large-scale direct shear device. The effects of different variables on the GCL and GCL-geomembrane interface shear strength are discussed, as well as the variability in the laboratory-obtained shear strength values and their relation to back-calculated shear strength values from failures. Specifically, the effects of normal stress, GCL reinforcement, geomembrane texturing and polymer type, moisture conditioning, and shear displacement rate are assessed through evaluation of data from the literature and from a database of commercial test results.

## 1 INTRODUCTION

Geosynthetic clay liners (GCLs) with geomembranes (GMs) placed on slopes as part of composite liner systems may be subject to a complex, time-dependent state of stresses. Stability is a major concern for side slopes in bottom liner or cover systems that include GCLs and GMs because of the wide range of commercially available GCL products, the change in behavior with exposure to water, variability in the quality of internal GCL reinforcement and GM texturing, and the low shear strength of hydrated sodium bentonite. Accordingly, proper project- and product-specific shear strength characterization is needed for the different materials and interfaces in composite liner systems.

A major concern when GCLs are placed in contact with GMs on steep slopes is the interface friction, which must be sufficiently high to transmit shear stresses generated during the lifetime of the facility. Shear stresses are typically generated in the field from static or seismic loads and waste decomposition. The need for a careful design of GCL-GM interfaces has been stressed by the failures generated by slip surfaces along liner interfaces, such as at the Kettleman Hills landfill

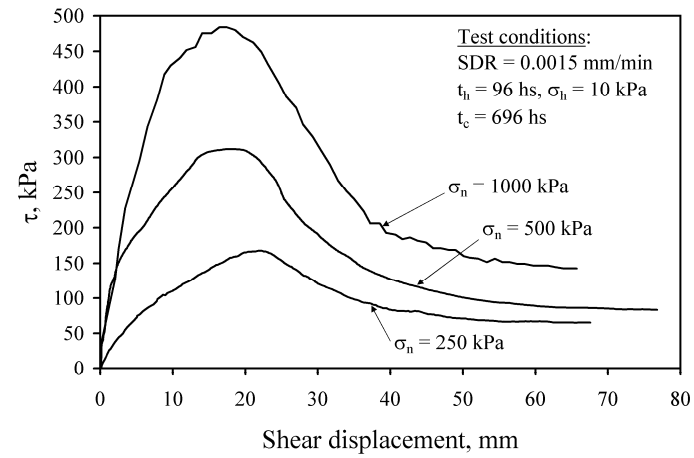


(a)

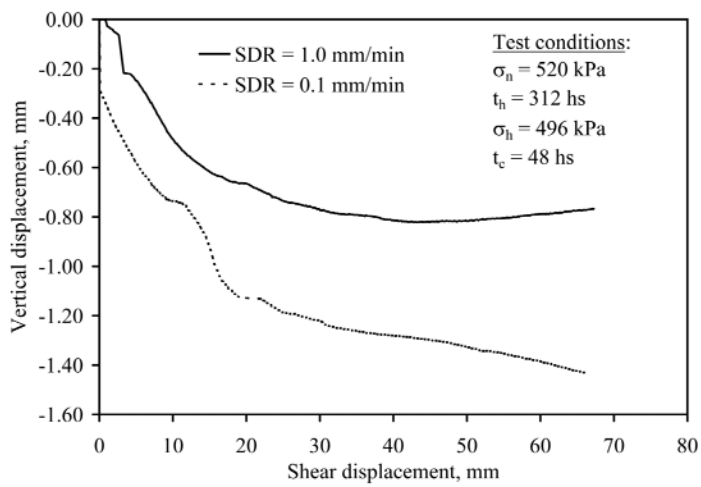


(b)

Figure 10: (a) Shear stress – shear displacement curves for needle-punched GCL sheared internally under different normal stresses; (b) Vertical displacement – Shear displacement curves

## 5.2 *Preliminary Shear Strength Overview*

Figure 11 shows GCL internal peak shear strength values $\tau_p$ reported in the literature. The wide range in shear strength reported by the different studies can be explained by differences in GCL reinforcement types, moisture conditioning procedures, shear displacement rates, as well as testing procedures and equipment used in the various studies, although significant variability is still apparent. Generally, reinforced GCLs show higher shear strength and greater variability than unreinforced GCLs.

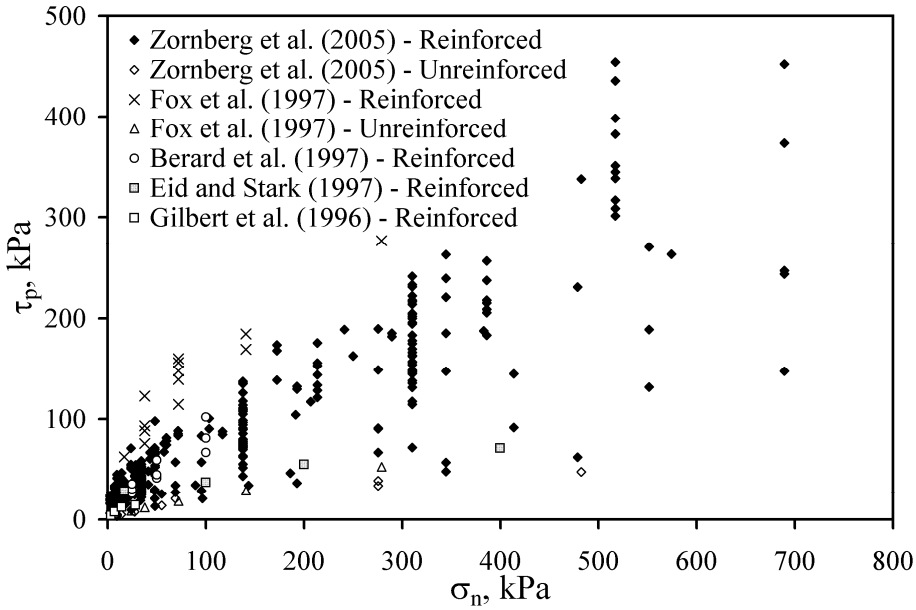


Figure 11: Overview of GCL internal peak shear strength values

## 5.3 *Variables Affecting GCL Internal Shear Strength*

### 5.3.1 *Effect of Normal Stress*

GCLs are frictional materials, so their shear strength increases with normal stress. Also, the internal reinforcements give the GCL strength at low normal stress. Accordingly, the GCL internal peak shear strength for a set of tests with the same conditioning procedures and shear displacement rate is typically reported using the Mohr-Coulomb failure envelope, given by:

$$\tau_p = c_p + \phi_p \tan \sigma_n \qquad (2)$$

where $\tau_p$ is the peak shear strength, $c_p$ is the cohesion intercept, $\sigma_n$ is the normal stress and $\phi_p$ is the interface friction angle. ASTM D6243 requires a minimum of three points [($\tau_{p1}$, $\sigma_{n1}$), ($\tau_{p2}$, $\sigma_{n2}$), ($\tau_{p3}$, $\sigma_{n3}$)] to define the peak or residual failure envelope for the given interface. Chiu and Fox (2004) and Zornberg *et al.* (2005) provide a range of internal peak shear strength parameters for different GCLs, hydration procedures, ranges of normal stresses, and shear displacement rates. Zornberg *et al.* (2005) also found that large-displacement shear strength was represented well by a linear failure envelope, although the cohesion intercept was typically negligible.

Most previous studies on GCL shear strength (Gilbert *et al.* 1996; Daniel and Shan 1993; Stark and Eid 1996; and Eid and Stark 1997, 1999) were for tests under low levels of normal stresses (typically below 200 kPa). Fox *et al.* (1998), Chiu and Fox (2004), and Zornberg *et al.* (2005) report shear strength values for a wider range in normal stresses, and indicate that linear failure envelopes do not represent the change in shear strength with normal stress. Accordingly, multi-linear or nonlinear failure envelopes are recommended. Gilbert *et al.* (1996) and Fox *et al.* (1998) used the model presented by Duncan and Chang (1970) to represent nonlinear trends in shear strength with normal stress, as follows:

$$\tau_p = \sigma_n \left[ \phi_0 - \Delta\phi \log\left( \frac{\sigma_n}{P_a} \right) \right] \tag{3}$$

where $P_a$ is the atmospheric pressure, $\phi_0$ is the secant friction angle at atmospheric pressure, and $\Delta\phi$ is the change in secant friction angle with the log of the normal stress normalized by $P_a$.

Figure 12 shows the trend in GCL internal peak shear strength with normal stress for different needle-punched GCLs. The results within each data set were obtained from direct shear tests with the same conditioning procedures and shear displacement rate. For tests under low normal stress ($\sigma_n$ < 100 kPa), a significant increase in peak shear strength is observed with normal stress, while for tests under high normal stress ($\sigma_n$ > 100 kPa), a less prominent increase in peak shear strength is observed.

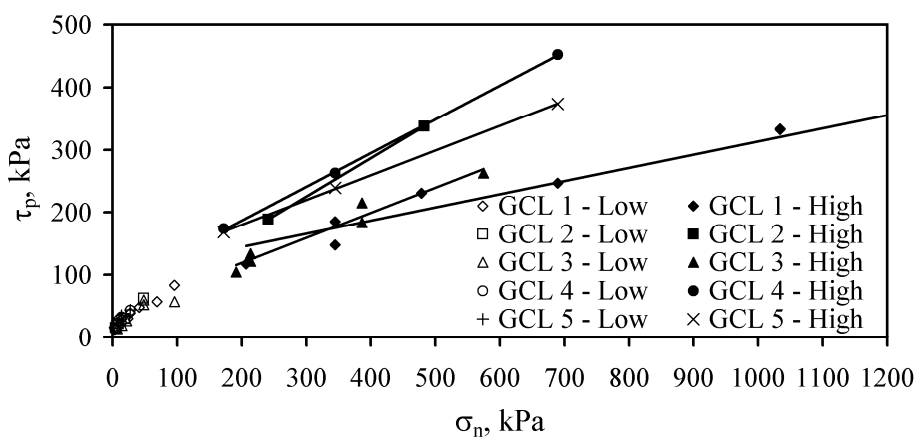


Figure 12: Normal stress effects on needle-punched GCL internal shear strength

The data in Figure 12 suggests that bilinear failure envelopes represent the data well for normal stresses under low normal stresses (< 100 kPa) and high normal stresses (>100 kPa). Zornberg *et al.* (2005) reported shear strength parameters for several bilinear failure envelopes. In addition, Chiu and Fox (2004) reported shear strength parameters for nonlinear failure envelopes. Both approaches tend

to represent the shear strength of GCLs over a wide range in normal stress. The change in GCL shear strength behavior with normal stress is important to consider when specifying normal stresses to define a failure envelope, which should always be within the range expected in the application.

The normal stress applied to a GCL may affect the lateral transmissivity of the carrier geotextiles. Depending on if the carrier geotextile is woven or nonwoven and the carrier geotextile compressibility, high normal stresses may lead to decreased lateral transmissivity of the carrier geotextiles. Combined with bentonite extrusion, the carrier geotextiles may not aid the dissipation of shear-induced pore water pressures under high normal stresses. The normal stress may also affect the strength of GCL reinforcements. Gilbert *et al.* (1996) reported that the resistance of fiber reinforcements to pullout from the carrier geotextiles increased with normal stress because of the frictional nature of the connections.

5.3.2 *GCL Reinforcement*

Table 1 shows typical shear strength parameters for different sets of GCLs reported by Zornberg *et al.* (2005). The peak shear strength calculated at a normal stress of 50 kPa, $\tau_{50}$, is also shown in Table 1 for comparison purposes. The peak internal shear strength of reinforced GCLs is significantly higher than that of unreinforced GCLs. The reinforced GCLs have a substantial intercept, while the unreinforced GCLs have a relatively low cohesion intercept and friction angle. The data in Table 1 indicates that needle-punched GCLs and thermally-locked GCLs have similar shear strength, while stitch-bonded GCLs have lower shear strength.

The difference between the needle-punched and thermal-locked GCLs may be explained by the pullout of reinforcements from the woven geotextile of the thermal-locked GCL during hydration and shearing (Lake and Rowe 2000). The fiber reinforcements in needle-punched GCLs are typically left entangled on the surface of the woven carrier geotextile, so significant swelling or shear displacement is required for pullout of the fibers from the carrier geotextile. On the other hand, the fibers in thermal-locked GCLs are melted together at the surfaces of the woven carrier geotextile. Stitch-bonded GCLs have less fiber reinforcement per unit area (stitches are typically at a 3-inch spacing), but the fiber reinforcements are continuous throughout the length of the GCL. Fox *et al.* (1998) and Zornberg *et al.* (2005) observed that the continuous fiber reinforcements in GCL *B* did not break during shearing, but instead the woven carrier geotextile ruptured at large shear displacements. The lower reinforcement density and mechanism of failure influences in the direct shear device leads to the low shear strength of these GCLs. Stitch-bonded GCLs are typically not used in practice. Table 1 also indicates that GCLs with nonwoven carrier geotextiles have similar shear strength at a normal stress of 50 kPa to woven carrier geotextiles. However, the greater friction angle of GCLs with woven carrier geotextiles leads to higher shear strength at high normal stresses for these GCLs.

Table 1: Shear strength parameters for GCL internal peak shear strength

| GCLdescription | Peak envelope | | $\tau_{50}$ (kPa) |
|---|---|---|---|
| | $c_p$ (kPa) | $\phi_p$ (Degrees) | |
| Reinforced GCLs | 40.9 | 18.0 | 57 |
| Unreinforced GCLs | 5.0 | 5.7 | 10 |
| Needle-punched GCLs | 40.5 | 19.5 | 61 |
| Stitch-bonded GCLs | 28.5 | 5.6 | 33 |
| Thermal-locked GCLs | 33.2 | 22.7 | 54 |
| W-NW needle-punched GCLs | 19.1 | 40.9 | 58 |
| NW-NW needle-punched GCLs | 35.0 | 24.5 | 58 |

Fox *et al.* (1998) found that the type of fiber reinforcement used in GCLs (needle-punched or stitch-bonded) has minor effect on the residual shear strength of GCL, although Zornberg *et al*. (2005) found that the type of fiber reinforcement still has an effect on the shear strength at a displacement of 75 mm.

Many studies have been conducted to investigate whether the internal shear strength of a needle-punched GCLs vary with the amount of needle punching per unit area of the GCL. Needle-punched GCLs are manufactured using a production line assembly which employs several threaded needles connected to a board (von Maubeuge and Ehrenberg 2000). As the lifetime of the needle-punching boards increases, more needles break and a lower density of fiber reinforcements may be apparent in the GCL with wear of the needle-punching board. The peel strength test (ASTM D6496) has been used as a manufacturing quality control test, as well as an index of the density (and possibly the contribution) of fiber reinforcements in needle-punched GCLs (Heerten *et al.* 1995, Eid and Stark 1999). Several studies have correlated the peak internal shear strength of needle-punched GCLs with peel strength (Berard 1997; Richardson 1997; Fox *et al.* 1998; Eid *et al.* 1999; Olsta and Crosson 1999; von Maubeuge and Lucas 2002; Zornberg *et al.* 2005). Figure 13 shows a comparison of the trends in peak shear strength of needle-punched GCLs with peel strength from several of these studies. An increase in peak shear strength is apparent in some of these data sets, although only Zornberg *et al.* (2005) used the same GCL, same conditioning procedures, and shear displacement rate. Overall, no trend is observed in this data.

Stark and Eid (1996) performed shear strength tests on reinforced GCLs with and without a sodium bentonite component (filled and unfilled, respectively) to find the effect of the reinforcement of the shear strength of reinforced GCLs. They found that the peak shear strength of unfilled GCLs was higher than that of filled GCLs, which indicates that the shear resistances of the sodium bentonite and the reinforcements are not additive. This trend may be due to pullout of the fiber reinforcements due to swelling of the bentonite during hydration. The pres-

# A TECHNICAL NOTE REGARDING INTERPRETATION OF COHESION AND FRICTION ANGLE IN DIRECT SHEAR TESTS

There is often confusion expressed in the geosynthetics industry over how laboratory direct shear results should be interpreted, specifically whether one should use both the friction angle and cohesion (or adhesion) parameters. The attached technical note from the April/May 2009 issue of Geosynthetics provides some guidance regarding this question, as well as several other issues related to direct shear results.

Please note that this article is not intended to replace education or experience and should only be used in conjunction with professional judgment. In the end, all data should be evaluated by an experienced practitioner qualified to use the test results properly.

TR-264
05/14

847.851.1800 | 800.527.9948

© 2014 CETCO. IMPORTANT: The information contained herein supersedes all previous printed versions, and is believed to be accurate and reliable. For the most up-to-date information, please visit www.CETCO.com. CETCO accepts no responsibility for the results obtained throught application of this product. CETCO reserves the right to update information without notice.

TR_264_AM_EN_201405_v1

CETCO®
An AMCOL Company
www.CETCO.com

# A technical note regarding interpretation of cohesion (or adhesion) and friction angle in direct shear tests

*By Richard Thiel*

## Introduction

Direct shear testing with geosynthetics is generally performed in accordance with ASTM D5321, *Standard Test Method for Determining the Coefficient of Soil to Geosynthetic or Geosynthetic to Geosynthetic Friction by the Direct Shear Method.* There is also a related standard, D6243, *Standard Test Method for Determining the Internal and Interface Shear Resistance of Geosynthetic Clay Liner by the Direct Shear Method.* This technical note applies to both equally.

## Interpreting lab results

There is often confusion expressed in the industry regarding how laboratory results should be interpreted, specifically: whether one should use both the friction angle and cohesion (or adhesion) parameters; whether cohesion should be ignored; whether secant friction angles are more appropriate; what to do if the data are nonlinear; and how the data should be interpolated or extrapolated.

The goal of this technical note is to provide some guidance to take the mystery out of these questions. In the end, all data should be evaluated by an experienced practitioner qualified to use the test results properly.

What this note will not do is go into the subtleties of requesting, setting up, calibrating, and performing a direct shear test. That would be the subject of additional articles.

| | |
|---|---|
| Material 1: | GSE 40 mil HDPE Tex / Tex (White side towards GCL) |
| Material 2: | Bentomat DN GCL (black side up) Roll # 00000481 |
| Substrate: | GSE 60 mil HDPE Tex-white / Tex-black (Black side toward GCL) |

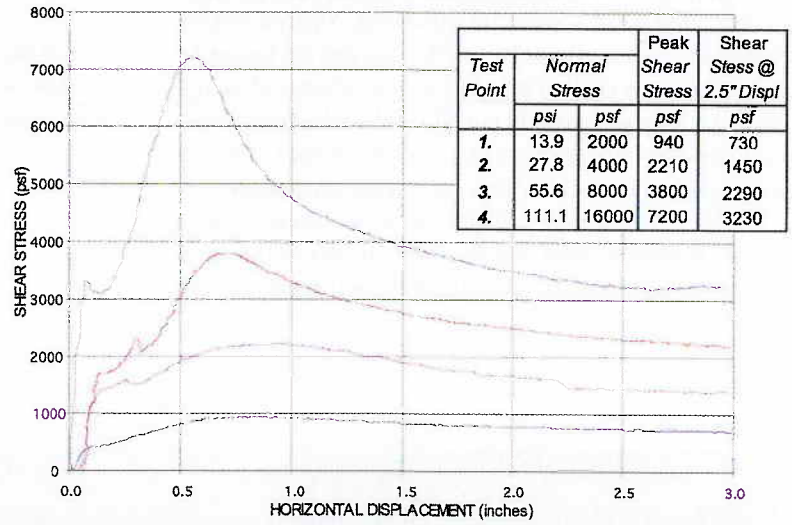


| Test Point | Normal Stress psi | Normal Stress psf | Peak Shear Stress psf | Shear Stess @ 2.5" Displ psf |
|---|---|---|---|---|
| 1. | 13.9 | 2000 | 940 | 730 |
| 2. | 27.8 | 4000 | 2210 | 1450 |
| 3. | 55.6 | 8000 | 3800 | 2290 |
| 4. | 111.1 | 16000 | 7200 | 3230 |

The "gap" between shear boxes was set at 80 mil (2.0 mm)
The test specimens were flooded during testing.
High Normal Stresses, >5psi (35 kPa) was applied using air pressure.
Low Normal Stresses, <5psi (35 kPa) was applied using dead weights.
The tests were terminated after 3.0"(75 mm) of displacement unless otherwise noted.
Tests were performed in general accordance with ASTM procedure D-5321 using a Brainard-Killman LG-112 direct shear machi
with an effective area of 12" x 12" (300 x300 mm).
Each specimen of 60 mil geomembrane was cut to 14" x 20" and clamped to the lower shear box. Avg. Asperity =0.025"
Each specimen of 40 mil geomembrane was cut to 14" x 16" and clamped to the upper shear box. Avg. Asperity =0.016"
Each GCL specimen was Hydrated for 48 hrs at the 250 psf, then placed, unclamped between upper & lower HDPEs
The grouped specimens were consolidated 16 hrs. under the specified normal stress, then sheared
Shearing occurred at the interface of the GCL's and 40 mil geomembrane specimens.
Extrusion of bentonite was noted on the surface of the 40 mil & white side of the GCL contact area for points 2,3 & 4
The Friction Angle and Adhesion (or Cohesion) results given here are based on a mathematically determined best fit line.
Further interpretation should be conducted by a qualified professional experienced in geosynthetic and geotechnical engineering.

This article will also not definitively describe how direct shear test data should be interpreted. That is the responsibility of a professional with specific expertise, and one article could never presume to cover all of the considerations that might apply to any unique design problem that might arise. That is why professionals are trained and mentored in basic geotechnical principles: so they can appropriately account for the various factors affecting a design and make appropriate decisions regarding test data interpretations.

The typical sequence of events related to direct shear testing includes the following:

**1.** An engineer requests a direct shear test series to obtain data to help solve a problem. The request should be very specific with regard to all the necessary details regarding

| Richard Thiel is a senior project manager at Vector Engineering Inc. in Grass Valley, Calif.

The Designer's Forum column is refereed by Greg Richardson, Ph.D., P.E., a principal at RSG & Associates, Raleigh, N.C., www.rsgengineers.com

sampling, specimen preparation and setup in the testing device, and test execution in accordance with both project-specific conditions and industry standards.

**2.** A competent and certified laboratory performs the test series in accordance with the request and the industry standard test method (e.g., ASTM D5321 or D6243). The laboratory reports results to the engineer.

**3.** The engineer interprets and applies the results to the project design.

**What we are measuring in the direct shear test is shear strength as a function of normal load. The test does not measure "friction" or "cohesion," as these are simply mathematical parameters derived from the laboratory test results.**

Ideally the engineer who originally specified and required the shear test would be the same one who reviews and interprets the results. Sometimes, such as in a third-party construction quality assurance (CQA) project, an engineer other than the original designer will commission and review the testing. Interactions with test laboratories and other engineers over time have shown that there are often misconceptions and misunderstandings related to the interpretation of direct shear test data. Thus, this article is intended to serve the purpose of helping project participants avoid confusion. The key point of this article is that what we are measuring in the direct shear test is shear strength as a function of normal load. The test does not measure "friction" or "cohesion," as these are simply mathematical parameters derived from the laboratory test results.

**Figure 1** presents shear test results of a 4-point test for an interface between a textured geomembrane and a reinforced GCL. Three shear points, each at a different normal stress, are the most common number of points used to run a test series, but the number of points could vary from as few as one, to perhaps as many as six points, depending on many factors beyond the scope of this article. The figure shows: (a) a table of the normal stresses vs. peak and large-displacement shear strengths measured at 2.5in. of displacement, (b) graphs of the shear stress vs. displacement measurements, and (c) notes describing test conditions and observations.

There is adequate information in this figure for a trained practitioner to evaluate and use the data. The laboratory has performed its duty, which is to measure and report the shear strength under specified normal stresses (we are simplifying the dis-

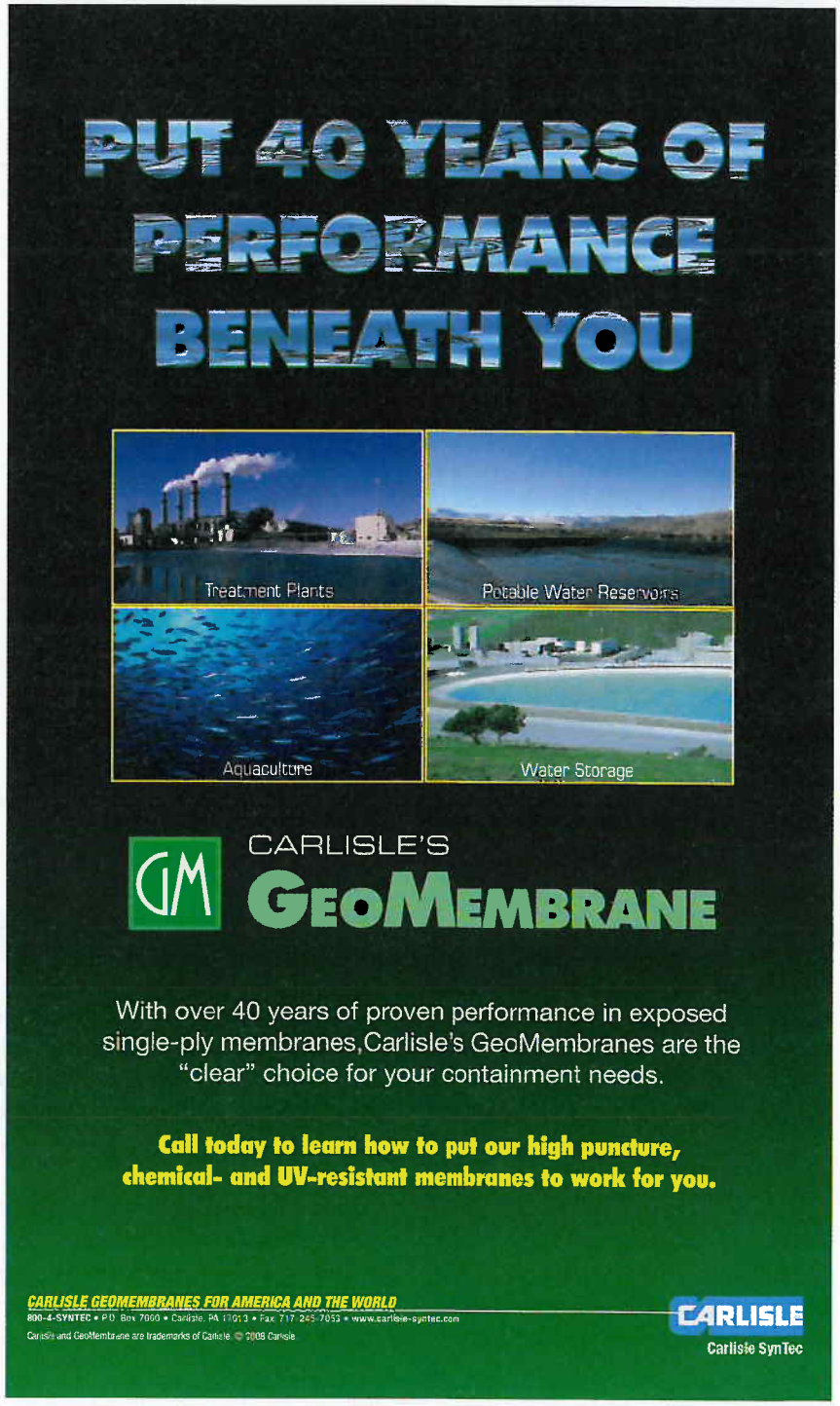

REFERENCE 7

cussion here by not elaborating on other factors such as hydration, consolidation, etc.), showing how the shear strength changed with displacement of the two surfaces, and providing descriptive and observational notes.

**Figure 2** shows additional information that can be provided by a laboratory in the form of a graph of the peak and large-displacement strengths plotted as a function of normal stress. Best-fit straight lines, called Mohr-Coulomb strength envelopes, named after the gentlemen who first publicized the relationship between shear strength and normal stress, have been drawn through the two sets (peak and large-displacement) of data points.

Equations can be written for these lines, as we learned in first-year algebra class, in the form of $y = mx + b$. In this case we define $y$ as the shear strength ($S$); $m$ as the slope of the line that we call the "coefficient of friction" and whose angle is *phi* ($\phi$), which we call the "friction angle" (and thus $\tan[\phi]$ is the slope of the line); $x$ is the normal stress ($N$); and $b$ is the y-intercept of the line that we call either "adhesion" ($a$, usually used for geosynthetics-only tests) or "cohesion" ($c$, usually used for tests involving soils, which will be used for the remainder of this article).

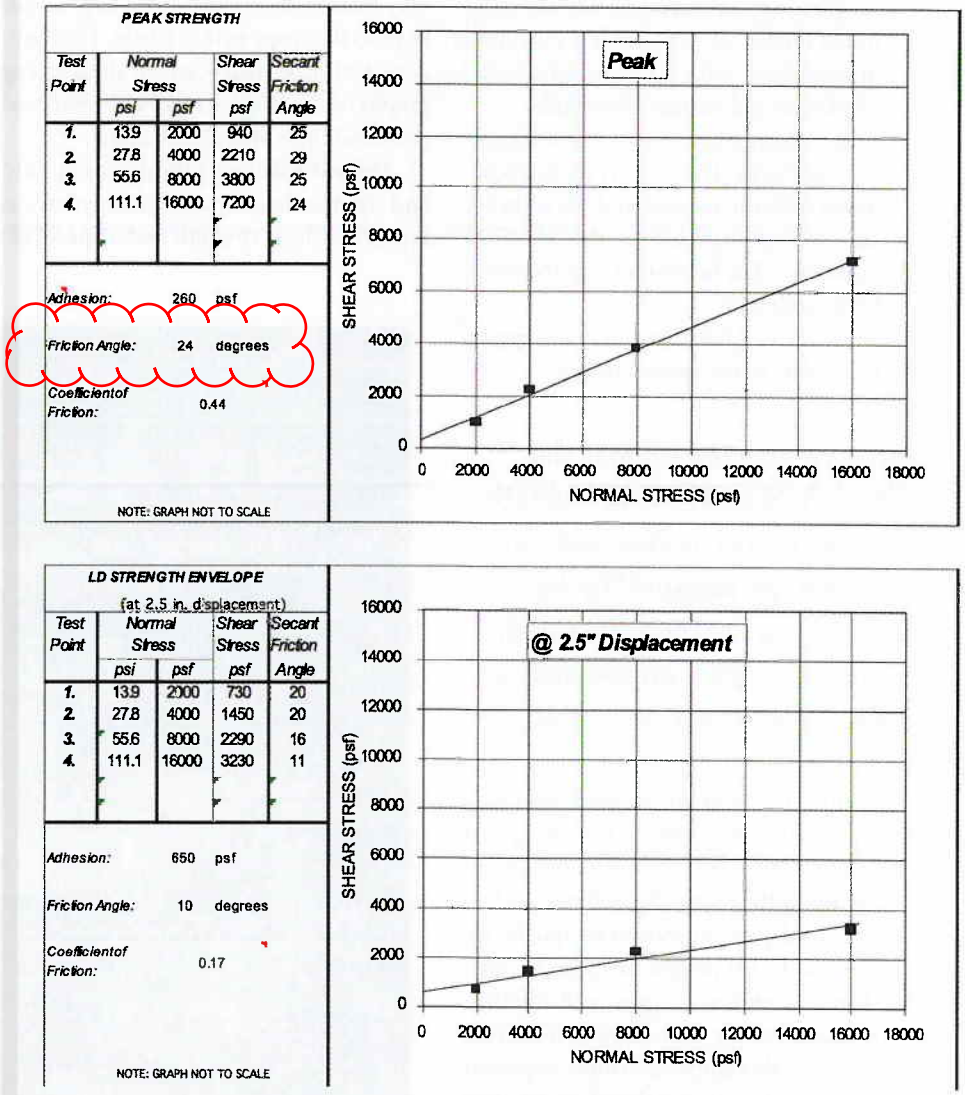


**Figure 2** | Example of supplemental data interpretation provided by the laboratory.

## Mohr-Coulomb

In geotechnical engineering, we write the Mohr-Coulomb equation for these lines as:

$$S = N \cdot \tan(\phi) + c$$

This equation is written for peak, large-displacement, or residual shear strength conditions. The fundamental points in this article regarding the presentation of the data in **Figure 2** include the following:

**1. The Mohr-Coulomb envelope should not be extrapolated beyond the limits of the normal stresses under which the testing was conducted.** To do so would never be conservative and, in fact, may be significantly nonconservative. The reason that simple extension-extrapolations of the Mohr-Coulomb envelope are nonconservative is presented in **Figure 3**. Most shear strength envelopes are truly curved (nonlinear). This tendency for a curved failure envelope is exaggerated in **Figure 3**, but can clearly be identified for the real-life strength envelopes presented in **Figure 2**, in particular for large-displacement conditions.

The Mohr-Coulomb model is merely a linear simplification of a portion of the entire envelope over a limited range of normal stresses. If testing were performed over a large enough range of normal stresses the curvature would become more apparent. True shear strength envelopes are found to be most accurately described by hyperbolic functions. Giroud et al. (1993) provides a good method to describe hyperbolic strength envelopes.

**2. The values of *phi* and *c* should be considered nothing more than mathematical parameters to describe the shear strength vs. normal stress *over the normal-load range the test was conducted.*** It is perhaps better not to think of "friction" and "cohesion" as real material properties, but simply as mathematical parameters to describe the failure envelope.

REFERENCE 7

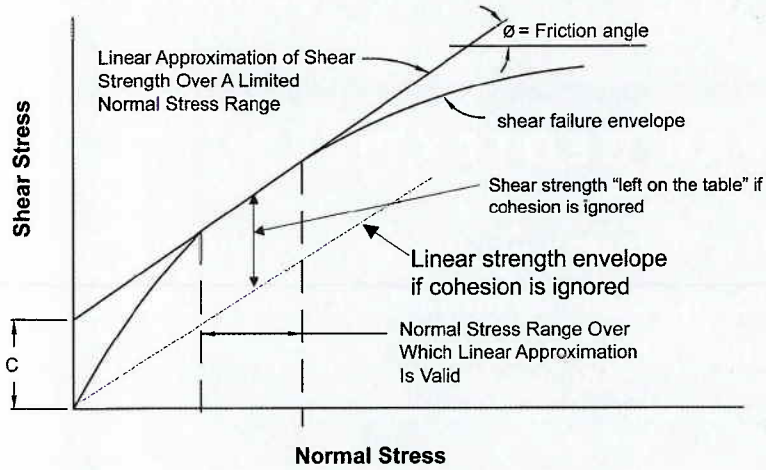


**Figure 3** | Exaggerated schematic of true curvilinear shear strength envelope, linear interpretation over a selected normal stress range, and the penalty for ignoring cohesion.

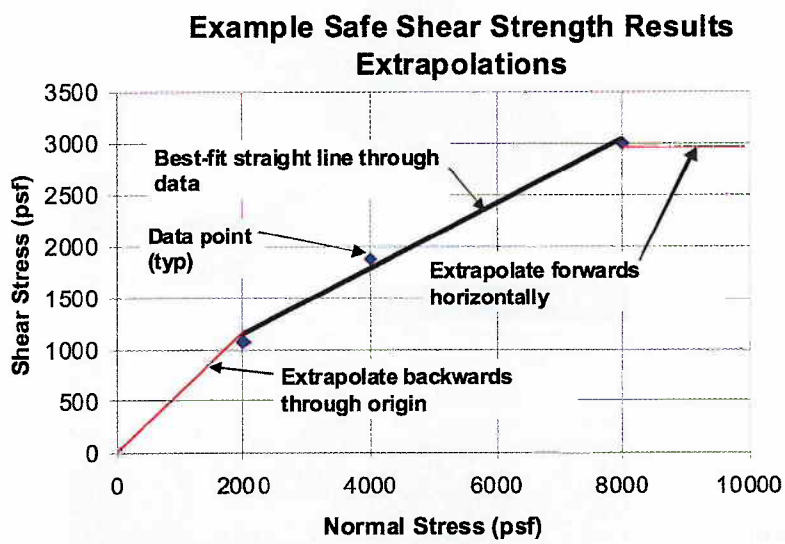


**Figure 4** | Example of safe shear strength extrapolation.

In geotechnical practice with soils, there are situations and examples where the cohesion parameter is evaluated separately from the friction parameter, but these are sophisticated considerations that involve very project-specific materials and conditions and should only be done by experienced professionals.

For many geosynthetic interfaces and in the context of many types of projects, there is absolutely no reason to dissociate the slope of the line from its y-intercept, and the shear strength should be taken as a whole in those cases. Other situations may occur, however, where it is appropriate, but those considerations are beyond the scope of this article.

**3.** In many, if not most, cases with geosynthetics where there is no reason to ignore the cohesion value, it is important to re-emphasize that shear strength should only be defined within the range of normal stresses for which the Mohr-Coulomb envelope was derived. Ignoring the cohesion may be unjustifiably penalizing the shear strength values that were measured in the test, as illustrated in **Figure 3**.

Using the cohesion value at normal stresses extrapolated below the range of testing, however, could have dire consequences on the safety of a design project. This problem may occur when designers consider only the operational or final build-out of a facility and they ignore the construction condition. Several failures have occurred during construction because of this. For example, an embossed geomembrane against a geotextile may perform well under high normal loads by providing a good friction angle and a modest y-intercept for operating and final build-out conditions. However, under the low normal loads experienced during construction of a thin soil veneer on a steep sideslope, testing might reveal that the adhesion extrapolated from the high-normal load results do not exist at low normal loads. In this case, a more aggressive texturing that exhibits a "Velcro®-effect" type of adhesion, or a very high friction angle, at low normal loads may be needed and should be verified at the proper normal loads.

**4. Figures 1** and **2** also report *secant* friction angles for each point. These are the angles of the straight lines from each point drawn back to the origin. A key concept regarding secant friction angles is that you should never extrapolate a secant angle line beyond the normal load for which it is measured. Secant values are conservative as long as the secant values are derived from a test whose normal stress was greater than the normal stresses of the design. They can quickly become nonconservative if the same friction angle is used for higher normal loads.

**5.** If users wish to extrapolate shear strength data, **Figure 4** illustrates the only "safe" way to accomplish this. Going from the low end of the Mohr-Coulomb envelope and extrapolating backward, the data can be extrapolated by drawing a straight line back to the origin. Going from the high end of the Mohr-Coulomb envelope and extrapolating forward, the data can be extrapolated by drawing a straight line